

# **Understanding Vortex Identification Criteria**

**A Thesis**

submitted to

Indian Institute of Science Education and Research Pune

in partial fulfillment of the requirements for the

BS-MS Dual Degree Programme

by

**Kirtikesh Kumar**



Indian Institute of Science Education and Research Pune

Dr. Homi Bhabha Road,

Pashan, Pune 411008, INDIA.

April, 2019

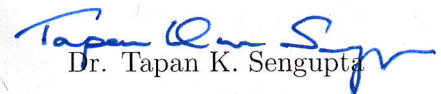
Supervisor: Dr. Tapan K. Sengupta

© Kirtikesh Kumar 2019

All rights reserved

# Certificate

This is to certify that this dissertation entitled 'Understanding Vortex Identification Criteria' towards the partial fulfilment of the BS-MS dual degree programme at the Indian Institute of Science Education and Research, Pune represents study/work carried out by Kirtikesh Kumar at Indian Institute of Technology, Kanpur under the supervision of Dr. Tapan K. Sengupta, Professor, Department of Aerospace Engineering, IIT Kanpur, during the academic year 2018-2019.

  
Dr. Tapan K. Sengupta

Committee:

Dr. Tapan K. Sengupta

Dr. Prasad Subramanian

This thesis is dedicated to my parents for their love, endless support and encouragement

# Declaration

I hereby declare that the matter embodied in the report entitled 'Understanding Vortex Identification Criteria', are the results of the work carried out by me at the Department of Aerospace Engineering, IIT Kanpur, under the supervision of Dr. Tapan K. Sengupta and the same has not been submitted elsewhere for any other degree.



Kirtikesh Kumar

# Acknowledgments

I wish to express my sincerest gratitude to Dr. Tapan K. Sengupta, Professor, Department of Aerospace Engineering, IIT Kanpur for his constant guidance during the thesis work. I would also like to thank all members of High-Performance Computing Lab, IIT Kanpur for their constant inputs and discussions, which helped me understand the topics discussed in this thesis. I would also like to thank Mr. Pushendra Sharma, PhD student, HPCL, IIT Kanpur for sharing the data of flow over a flat plate for analysis in this thesis.

I wish to thank my parents and all my friends at IIT Kanpur and IISER Pune for their moral support during my stay at IIT Kanpur, without which I would not have been able to complete my thesis project at IIT Kanpur.

I would like to acknowledge the High-Performance Computing facility at IIT Kanpur for allowing me to use their HPC10 cluster for running all the numerical analysis code.

# Abstract

In this thesis two new criteria used for instability analysis based on equations for disturbance mechanical energy (Sengupta et al.: Vortex-induced instability of an incompressible wall-bounded shear layer. *Journal of Fluid Mechanics*, 493:277–286, 2003) and disturbance enstrophy (Sengupta et al.: An enstrophy-based linear and nonlinear receptivity theory. *Physics of Fluids*, 30(5):054106, 2018) are discussed and compared with commonly used  $Q$ -criterion (Hunt, Wray and Moin: Eddies, streams, and convergence zones in turbulent flows, CTR Report, Stanford Univ., 1988) and  $\lambda_2$ -criteria (Jeong and Hussain: On the identification of a vortex, *J. Fluid Mech.*, 285, 69-94, 1995) for vortex identification for a zero pressure gradient flow over a flat plate. The criteria used for instability analysis are derived directly from Navier-Stokes equation for incompressible flow without any assumptions. We show the superiority of these new criteria over the commonly used  $Q$ - and  $\lambda_2$ -criteria in distinguishing between flow before and after the formation of a turbulent spot. Criteria based on disturbance enstrophy equation is also used along with instantaneous vorticity to explain the initiation of flow transition. As the commonly used vortex identification criteria are just mathematical constructs without any clear physical meaning, an attempt is made to correlate them with rate of change of disturbance enstrophy using a point search algorithm. A similarity is observed between instantaneous vorticity and DETE for all times. Scale factors are then extracted to explain this similarity.

# Contents

<b>Abstract</b>	<b>vi</b>
<b>1 Introduction</b>	<b>1</b>
1.1 Requirements for a vortex core . . . . .	1
1.2 Circular path-lines or streamlines . . . . .	2
1.3 Vorticity . . . . .	2
1.4 Pressure minimum criteria . . . . .	3
1.5 Q-Criteria . . . . .	3
1.6 $\lambda_2$ -criteria . . . . .	4
1.7 Problems with pressure minimum criteria . . . . .	5
1.8 Rortex . . . . .	6
1.9 Disturbance Enstrophy Transport Equation . . . . .	9
1.10 Disturbance Mechanical Energy . . . . .	10
<b>2 Methods</b>	<b>12</b>
2.1 Flow Details . . . . .	12
2.2 Calculation of different criteria . . . . .	14
2.3 Correlation Methodology . . . . .	15

<i>CONTENTS</i>	viii
<b>3 Results and Discussions</b>	<b>17</b>
3.1 Comparison of different criteria . . . . .	17
3.2 Evolution of the flow . . . . .	18
3.3 Correlation of criteria . . . . .	19
<b>4 Summary and Conclusion</b>	<b>21</b>
<b>5 Figures</b>	<b>23</b>



# List of Figures

1.1	Deformation of fluid element . . . . .	8
2.1	Computational domain of the flat plate flow . . . . .	13
5.1	comparison between various criteria for $t = 25.3$ . . . . .	24
5.2	comparison between various criteria for $t = 29.3$ . . . . .	25
5.3	Slices for $t = 25.1$ to $25.5$ at $z = 0.1875$ . . . . .	26
5.4	Slices for $t = 25.7$ to $26.1$ at $z = 0.1875$ . . . . .	27
5.5	Slices for $t = 26.3$ to $26.9$ at $z = 0.1875$ . . . . .	28
5.6	Slices for $t = 27.1$ to $27.5$ at $z = 0.1875$ . . . . .	29
5.7	Slices for $t = 27.7$ to $28.1$ at $z = 0.1875$ . . . . .	30
5.8	Slices for $t = 28.3$ to $28.7$ at $z = 0.1875$ . . . . .	31
5.9	Slices for $t = 25.1$ to $25.5$ at $z = 0.0625$ . . . . .	32
5.10	Slices for $t = 25.7$ to $26.1$ at $z = 0.0625$ . . . . .	33
5.11	Slices for $t = 26.3$ to $26.9$ at $z = 0.0625$ . . . . .	34
5.12	Histogram of DME and Vorticity for $DETE = 100 \pm 5$ at $t = 27.1$ . . . . .	35
5.13	Histogram of $\lambda_2$ - and $Q$ - criteria for $DETE = 100 \pm 5$ at $t = 27.1$ . . . . .	35
5.14	correlation of various criteria w.r.t $DETE$ at $t = 27.1$ . . . . .	36

5.15	correlation of various criteria w.r.t DETE . . . . .	37
5.16	correlation of various criteria w.r.t DETE . . . . .	38
5.17	correlation of various criteria w.r.t DETE . . . . .	39
5.18	correlation of various criteria w.r.t DETE . . . . .	40
5.19	correlation of various criteria w.r.t DETE . . . . .	41
5.20	correlation of various criteria w.r.t DETE . . . . .	42
5.21	correlation of various criteria w.r.t DETE . . . . .	43
5.22	correlation of various criteria w.r.t DETE . . . . .	44
5.23	correlation of various criteria w.r.t DETE . . . . .	45
5.24	correlation of various criteria w.r.t DETE . . . . .	46
5.25	correlation of various criteria w.r.t DETE . . . . .	47
5.26	similarity of $ \vec{\omega} $ with DETE for $27.1 \leq t \leq 29.3$ . . . . .	48
5.27	variation of $\alpha$ and $\beta$ of exponential fit with time . . . . .	48
5.28	exponential fit of scaled $ \vec{\omega} $ vs scaled DETE. . . . .	48

# Chapter 1

## Introduction

Turbulence is viewed as a tangle of vortices, with vorticity dynamics playing a vital role in its understanding. The problem in understanding of vortices and their dynamics is the absence of a clear definition of a vortex. It is generally understood that a vortex must be a region of fluid rotating about an axis. There have been various criteria proposed to educe vortical structures most commonly used of which being  $\lambda_2$  and  $Q$ -criteria. More recent criteria like Rortex,  $\lambda_\rho$ , DME and DETE also attempt to extract vortical structures. A review of some existing criteria for vortex identification is available in [4]. In this thesis, we attempt to compare some of these criteria and their salient features by using flow over a flat-plate at high Reynolds numbers. We start with stating the minimum requirements for a vortex in § 1.1 followed by a brief description of some criteria for identifying a vortex in §1.2-§1.10. This is followed by a brief description of simulation of the flow in §2.1, calculation method of each criteria used in §2.2 and the adopted correlation methodology in §2.3. Chapter 3 discusses the results obtained.

### 1.1 Requirements for a vortex core

As discussed before, though a vortex core does not have any universally agreed upon mathematical definitions, a region of flow is required to satisfy certain conditions to be considered as a vortex. These criteria are based on the intuitive understanding of a vortex

and reference frames and are necessary but not sufficient. Stated in [8] these requirements are:

1. The net vorticity inside a vortex must be non-zero.
2. A vortex must be galilean invariant.

the second requirement is imposed as [10] stated that turbulence does not have any distinguished frame of reference, thus any reference frame used to observe the flow must agree upon the coherent structures observed. In regards to this, [6] extended the requirement from galilean invariance to objectivity, i.e., a vortex remains invariant under any general transformation of a reference frame, including rotation. As stated in [4] this condition is not required in most applications, and galilean invariance of the structures identified is sufficient. Initial criteria to identify vortices were based on qualitative understanding of a vortex, and had various drawbacks as are explained in [8] and discussed here for the sake of completeness.

## 1.2 Circular path-lines or streamlines

This method proposed in [10] was based on the understanding that a particle in the vicinity of a vortex will tend to revolve around it, thus resulting in a closed or spiral path-line. A drawback of using a path-line was that the particle may not complete a full revolution about the axis during the lifetime of a vortex. This can happen if the vortex undergoes transition due to non-linear processes before the particle completes a full revolution. This drawback does not occur if streamlines are used instead of path-lines. The usage of streamlines however has a major problem of being frame variant. Thus two vortices in the same flow convecting with different velocities will not be seen in the same reference frame.

## 1.3 Vorticity

In a flow in absence of shear, presence of vorticity is a signature of a vortex. This however is not true if the flow has shear included, as shear provides a large vorticity bank

even in the absence of a vortex.

## 1.4 Pressure minimum criteria

This is based on the understanding that the centrifugal force on a particle revolving around the vortex will be balanced by the pressure force. This was used to develop the Q-criteria by Hunt et al. [2]. The problem with this criteria however lies in the fact that pressure can have a minimum in regions without any vorticity as in a flow with unsteady irrotational axisymmetric motion with a stagnation point (ex.  $u_r = -\alpha(t)r$ ,  $u_\theta = 0$ ,  $u_z = 2\alpha(t)z$  where solving euler equation gives pressure as  $p = (\dot{\alpha}(t) - \alpha(t)^2)\frac{1}{2}r^2 + (-\dot{\alpha}(t) - \alpha(t)^2)z^2$ ) where the pressure can have a minimum due to the unsteady strain rate  $\alpha(t)$  and its time rate of change  $\dot{\alpha}(t)$ . Another problem with this criteria is when either the centrifugal force or the pressure force is balanced by viscous force as in the case of karman vortex pump or very low Re stokes flow, which can lead to wrong interpretation of the structures educed using the pressure minimum criteria.

## 1.5 Q-Criteria

Q-criteria, proposed by Hunt et al. [2], identified different “zones” of flow using different threshold values of the second invariant ( $Q$ ) of the gradient of velocity tensor ( $\nabla\mathbf{u}$ ), defined as:

$$Q = \frac{1}{2}[(tr(\nabla\mathbf{u}))^2 - tr(\nabla\mathbf{u})^2] = \frac{1}{2}(u_{i,i}^2 - u_{i,j}u_{j,i}) \quad (1.1)$$

The first term drops out for an incompressible fluid. Thus Eq.(1.1) becomes:

$$Q = -\frac{1}{2}u_{i,j}u_{j,i} \quad (1.2)$$

which can be related to pressure poisson equation for incompressible flows by:

$$\nabla^2 P = 2\rho Q \quad (1.3)$$

Thus a positive value of  $Q$  would mean a sink of pressure, and negative  $Q$  is a source of pressure. A vortex (called eddying zone in [2]) is identified as a connected region with positive  $Q$  and a minimum of pressure. Thus the  $Q$ -criteria is essentially identifying a minimum of pressure at the location of a pressure sink. It can be seen from Eq.(1.3) that  $Q$ -criteria is independent of effects of viscous and unsteady straining terms in the pressure minimum criteria. In common practice the minimum of pressure is ignored and only positive  $Q$  is used to identify a vortex, as data for pressure is not collected at all locations. This however has the problem that pressure need not have a minimum inside the region of pressure sink, i.e. pressure can have a minimum at the boundary of this region. Thus there is no explicit connection between region of pressure sink and a pressure minima.

$Q$  can also be interpreted as a local excess of rotation rate with respect to strain rate. This can be done by writing  $Q$  in terms of rotation rate tensor ( $\Omega = \frac{1}{2}(\nabla\mathbf{u} - \nabla\mathbf{u}^T)$ ) and strain rate tensor ( $\mathbf{S} = \frac{1}{2}(\nabla\mathbf{u} + \nabla\mathbf{u}^T)$ ) as:

$$Q = \frac{1}{2}tr(\Omega\Omega^T - \mathbf{S}\mathbf{S}^T) \quad (1.4)$$

Eq.(1.4)is true only for an incompressible fluid, and can be derived by taking the trace of the gradient of Navier-Stokes equation, as shown in [8], and in the next section.

## 1.6 $\lambda_2$ -criteria

Though the use of pressure minimum suffers from the flaws discussed above, Jeong & Hussain [8] used this as a starting point to define this criteria. While doing this the contributions from unsteady irrotational straining and viscous terms were neglected. This criteria can be derived by taking the gradient of Navier-Stokes equation:

$$a_{i,j} = -\frac{1}{\rho}P_{,ij} + \nu u_{i,jkk} \quad (1.5)$$

where  $a_{i,j}$  is the gradient of acceleration term, and  $P_{,ij}$  is the pressure hessian. The acceleration term can be written in terms of velocity gradient tensor which can be further broken down in terms of rotation rate tensor ( $\Omega$ ) and strain rate tensor ( $\mathbf{S}$ ) giving:

$$\begin{aligned}
-\frac{1}{\rho}P_{,ij} = & \left( \frac{D}{Dt}\Omega_{ij} + \Omega_{ik}\mathbf{S}_{kj} + \mathbf{S}_{ik}\Omega_{kj} - \nu\Omega_{ij,kk} \right) \\
& + \left( \frac{D}{Dt}\mathbf{S}_{ij} + \Omega_{ik}\Omega_{kj} + \mathbf{S}_{ik}\mathbf{S}_{kj} - \nu\mathbf{S}_{ij,kk} \right)
\end{aligned} \tag{1.6}$$

The first four terms in parenthesis in Eq.(1.6) are antisymmetric, while the next four terms are symmetric. The antisymmetric part is the vorticity transport equation in tensor form and hence, is analytically equal to zero thus Eq.(1.6) becomes:

$$\frac{D}{Dt}\mathbf{S}_{ij} - \nu\mathbf{S}_{ij,kk} + (\Omega_{ik}\Omega_{kj} + \mathbf{S}_{ik}\mathbf{S}_{kj}) = -\frac{1}{\rho}P_{,ij} \tag{1.7}$$

The first term of Eq.(1.7) is the unsteady irrotational straining term while the second term is a viscous term which is neglected from the equation. The second derivative test is then applied to the remaining equation for the pressure hessian. This requires two positive eigenvalues of  $P_{,ij}$  tensor, which translates to two negative eigenvalues of  $(\Omega^2 + \mathbf{S}^2)$  tensor. Let  $\lambda_1, \lambda_2, \lambda_3$  be the three eigenvalues of  $(\Omega^2 + \mathbf{S}^2)$ , such that  $\lambda_1 \geq \lambda_2 \geq \lambda_3$ . Then ensuring  $\lambda_2 \leq 0$  ensures two negative eigenvalues of  $(\Omega^2 + \mathbf{S}^2)$  and thus two positive eigenvalues of  $P_{,ij}$ . Hence a vortex is identified as a connected region with  $\lambda_2 \leq 0$ .

Taking the trace of Eq.(1.7) and using  $tr(\mathbf{S}) = 0$ ,  $\Omega\Omega = -\Omega\Omega^T$  and Eq. (1.3), we get Eq.(1.4). Hence the relation between  $\lambda_2$ -criteria and Q-criteria is:

$$Q = -\frac{1}{2}(\lambda_1 + \lambda_2 + \lambda_3) \tag{1.8}$$

Both  $\lambda_2$ -criteria and Q-criteria give the same results for a planar flow.

## 1.7 Problems with pressure minimum criteria

As was stated in the section on  $\lambda_2$ -criteria, the unsteady straining and viscous terms can lead to spurious appearance and disappearance of pressure minima in a flow. Thus  $\lambda_2$ -criteria drops these terms when considering a pressure minimum. Q-criteria on the other hand does not suffer from problems caused by these terms, as they do not contribute.

Another problem is the choice of correct isosurface value for visualization of the flow. It is observed that for isosurface values close to zero the number of structures and their connectivity with other structures increases. Thus depending on isosurface value chosen, two structures may or may not be connected. The contribution from the extra structures identified at very low isosurface values of these criteria, cannot be understood as a clear physical meaning is not assigned to these structures. In §3.3 an attempt is made to give a physical meaning to these criteria by correlating with respect to another criteria.

It is a common practice to visualize the isosurfaces at 'zero' value. This practice should be avoided if possible as zero is the limiting case for both the discussed criteria, hence it is not necessary that the 'zero' isosurface signify a distinction between region containing vortices and those not containing it, It could be a saddle region, which would appear as a vortex if it forms a connected region. This is a point also discussed in [3] where it is shown that the usage of the isosurface value of '0' in  $\lambda_2$ -criteria results in identification of spurious structures.

The criteria which identify vortices as regions of pressure minimum do not take into account all the contributions to pressure, and hence do not give a complete picture of the flow. The eigenvalue based criteria identify vortices as region of two complex eigenvalues of the  $\nabla \mathbf{u}$  tensor. These criteria are more computationally expensive ( $\lambda_2$ -criteria uses symmetric matrix to make things simple), and do not explain the physical significance of the eigenvalues and eigenvectors together. To counter this problem, we discuss three new criteria that aim to represent the flow without losing on any part of the governing Navier-Stokes equation.

## 1.8 Rortex

Tian et.al [14] & Liu et.al [9] proposed defining vortices as connected regions with rigid rotation about an axis (vortex core). In this method the vorticity vector is decomposed into a component due to rigid rotation of the fluid and a non-rotating component which includes shearing, stretching and compression. It should be noted that these two components are not orthogonal due to non-linearity of the governing Navier-Stokes equation. The rigid rotation component of vorticity gives the direction of local rotation axis and the magnitude of rigid



rotation of fluid in a plane perpendicular to the rotation axis.

In a coordinate system 'XYZ' with origin at 'O', a local rotation axis 'Z' at point 'O' is defined as an axis such that the rotational motion in a small neighborhood around the point is confined to the plane 'XY' perpendicular to this axis. Thus there can be no axis of rotation in the XY plane. This can be achieved by finding a coordinate system such that:

1.  $\frac{\partial U}{\partial Z} = 0$  or  $\frac{\partial W}{\partial X} = 0$ , for no rotation about the Y axis
2.  $\frac{\partial V}{\partial Z} = 0$  or  $\frac{\partial W}{\partial Y} = 0$ , for no rotation about the X axis

Let  $\mathbf{r} = r_x \hat{\mathbf{i}} + r_y \hat{\mathbf{j}} + r_z \hat{\mathbf{k}}$  be the local rotation axis in the global 'xyz' frame of reference. Then a transformation of  $\nabla \mathbf{u}$  in the global frame to  $\nabla \mathbf{U}$  in the local 'XYZ' frame with Z as the axis of rotation can be done using quaternions approach as:

$$\nabla \mathbf{U} = \mathbf{M} \nabla \mathbf{u} \mathbf{M}^{-1} \quad (1.9)$$

Here  $\mathbf{M}$  is the transformation matrix from 'xyz' to 'XYZ' found by schur decomposition of  $\nabla \mathbf{u}$ , with

$$\mathbf{M} \mathbf{r} = \begin{bmatrix} 0 \\ 0 \\ 1 \end{bmatrix} \quad (1.10)$$

The transformation from global 'xyz' coordinate system to local 'XYZ' coordinate system converts the local fluid rotation from 3-D to 2-D, confined to the XY plane in the transformed 'XYZ' coordinate system. The presence of a local rotation axis however does not imply that there is rigid rotation about this axis. Rigid rotation requires all points on the XY-plane in a small neighborhood of the axis to rotate about it with the same angular velocity. It can be seen from Fig:(1.1) that deformation of fluid element can be classified into three types using the derivatives of velocity in the XY plane as:

$$g_Z = -\frac{\partial U}{\partial Y} \frac{\partial V}{\partial X} \quad (1.11)$$

1. pure shearing if  $g_Z = 0$

2. irrotational deformation if  $g_z < 0$
3. rotational deformation if  $g_z > 0$

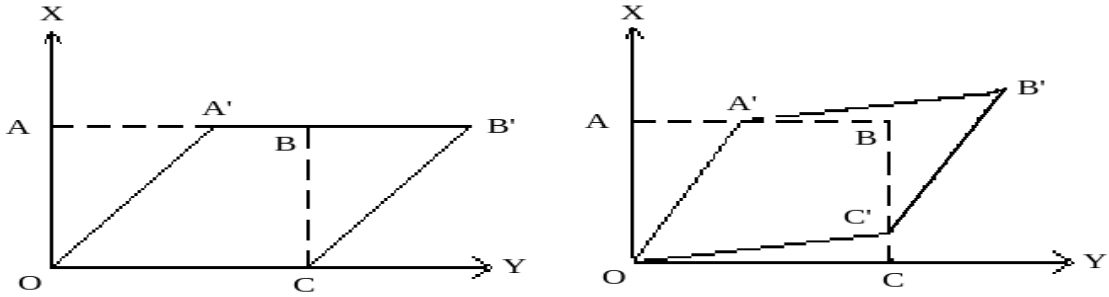


Figure 1.1: Deformation of fluid element due to gradients in XY-plane.(a)shear deformation, (b)rotational deformation

In a 2-D flow, the vorticity is an invariant under rotation of axis in the plane of flow, but the derivatives  $\frac{\partial U}{\partial Y}$  and  $\frac{\partial V}{\partial X}$  need not be invariants. Thus to ensure that  $g_z$  does not change sign if the local XY-plane is rotated about Z-axis, we calculate  $g_z$  as a function of rotation of XY-plane about Z-axis. For solid body rotation to be present,  $g_z$  should be positive for all such rotations. The new velocity gradient tensor after rotation of XY-plane about Z-axis, by an angle  $\theta$  is given by:

$$\nabla \mathbf{U}_\theta = \mathbf{P} \nabla \mathbf{U} \mathbf{P}^{-1} \quad (1.12)$$

Where  $\mathbf{P}$  is the transformation matrix for rotation about Z-axis.the magnitude of rigid rotation is given by twice the minimum angular velocity around the point i.e The Rortex ( $\mathbf{R}$ ) is given by.

$$\mathbf{R} = r \mathbf{r} \quad (1.13)$$

$$r = \begin{cases} 2 \cdot \min \left\{ \left| \frac{\partial U}{\partial Y} \right|_\theta, \left| \frac{\partial V}{\partial X} \right|_\theta \right\} & \text{if } |\beta| > |\alpha| \\ 0 & \text{if } |\beta| < |\alpha| \end{cases} \quad (1.14)$$

The significance of Rortex can be explained using eigenvalue-eigenvector analysis as done in [5]. The regions with non-zero magnitudes of Rortex correspond to regions with complex eigenvalues of velocity gradient tensor. The complex eigenvalues of  $\nabla \mathbf{u}$  are regions of circulating flow, which can be considered as a vortex as discussed in §1.2.

## 1.9 Disturbance Enstrophy Transport Equation

This is a new method proposed by Sengupta et.al [22] for stability analysis. This method can also be used for identification of vortices. Though this method does not use  $\nabla \mathbf{u}$  tensor, it will be shown subsequently that this method satisfies both requirements for a vortex as set by [8].

The vorticity transport equation in non-dimensional form is written as:

$$\frac{\partial \boldsymbol{\omega}}{\partial t} + (\mathbf{u} \cdot \nabla) \boldsymbol{\omega} = (\boldsymbol{\omega} \cdot \nabla) \mathbf{u} + \frac{1}{Re} \nabla^2 \boldsymbol{\omega} \quad (1.15)$$

$\boldsymbol{\omega}$  is the vorticity. Taking a dot product of  $\boldsymbol{\omega}$  with Eq.(1.15), we get the enstrophy transport equation:

$$\frac{\partial \Omega}{\partial t} + u_j \frac{\partial \Omega}{\partial x_j} = 2\boldsymbol{\omega}_i \boldsymbol{\omega}_j \frac{\partial u_i}{\partial x_j} + \frac{1}{Re} \frac{\partial^2 \Omega}{\partial x_j \partial x_j} + \frac{2}{Re} \frac{\partial \boldsymbol{\omega}_i}{\partial x_j} \frac{\partial \boldsymbol{\omega}_i}{\partial x_j} \quad (1.16)$$

here  $i, j = 1, 2, 3$  are coordinate indices.  $\Omega = \boldsymbol{\omega} \cdot \boldsymbol{\omega}$  is the enstrophy (Not to be confused with  $\boldsymbol{\Omega}$  of rotation rate matrix). The first term on the LHS is the vortex stretching term, the second term on LHS is the dissipation of  $\Omega$  and the third term on LHS is the dissipation of transport of  $\Omega$ .

The Enstrophy can be written as sum of a mean and disturbance from mean as  $\Omega = \Omega_m + \varepsilon \Omega_d$ , where  $\varepsilon$  represents a small value. Velocity and vorticity can similarly be broken down into  $\mathbf{u} = \mathbf{u}_m + \varepsilon \mathbf{u}_d$  and  $\boldsymbol{\omega} = \boldsymbol{\omega}_m + \varepsilon \boldsymbol{\omega}_d$ . Substituting velocity, vorticity and enstrophy in terms of mean and disturbance quantities into enstrophy transport equation, subtracting the equation for mean values from Eq.(1.16) and linearizing by retaining terms of order  $\varepsilon$  gives the linear form of Disturbance Enstrophy Transport Equation

$$\frac{D\Omega_d}{Dt} = \left[ \left\{ \boldsymbol{\omega}_{im} \boldsymbol{\omega}_{jm} \frac{\partial u_{id}}{\partial x_j} + \boldsymbol{\omega}_{im} \boldsymbol{\omega}_{jd} \frac{\partial u_{im}}{\partial x_j} + \boldsymbol{\omega}_{id} \boldsymbol{\omega}_{jm} \frac{\partial u_{im}}{\partial x_j} \right\} + \frac{1}{Re} \frac{\partial^2 \Omega_d}{\partial x_j \partial x_j} - \frac{2}{Re} \frac{\partial \boldsymbol{\omega}_{im}}{\partial x_j} \frac{\partial \boldsymbol{\omega}_{id}}{\partial x_j} \right] \quad (1.17)$$

To show the galilean invariance of Eq.(1.17), we change to a coordinate system moving with a constant velocity  $\mathbf{c}$  with respect to original system as  $\mathbf{x} \rightarrow \mathbf{x}' + \mathbf{c}t$ . The various

quantities in Eq.(1.17) change as:

$$\begin{aligned}\frac{\partial}{\partial x_j} &= \frac{\partial x'_j}{\partial x_j} \frac{\partial}{\partial x'_j} + \frac{\partial t}{\partial x_j} \frac{\partial}{\partial t} = \frac{\partial}{\partial x'_j} \\ \frac{\partial}{\partial t} &= \frac{\partial}{\partial t} \\ \mathbf{u} &= \mathbf{u}' + \mathbf{c} \\ \omega_j &= \omega'_j \\ \Omega &= \Omega\end{aligned}$$

Substituting the above relations to transform the coordinate system for Eq.(1.17) gives the galilean invariant equation. Thus it is seen that DETE provides a galilean invariant quantity to use for stability analysis. As this criteria will have a non zero value in locations of non-zero vorticity, this criteria also meets both the minimum requirements from a vortex identification criteria as discussed in §1.1. It is also seen that pressure forcing does not appear in this equation, hence this criteria does not suffer from the problems caused by unsteady straining and viscous terms as discussed earlier. This allows us to include the effects of these terms, giving a complete picture of the flow.

## 1.10 Disturbance Mechanical Energy

Sengupta et.al [12] derived an equation for total mechanical energy from the incompressible Navier-Stokes equation for stability analysis in transitional flows. This equation gives the regions of source and sink of total mechanical energy. The Navier-Stokes equation can be written as

$$\frac{\partial \mathbf{u}}{\partial t} - \mathbf{u} \times (\nabla \times \mathbf{u}) = -\frac{1}{\rho} \nabla P - \frac{1}{2} \nabla |\mathbf{u}|^2 + \nu \nabla (\nabla \cdot \mathbf{u}) - \nu \nabla \times (\nabla \times \mathbf{u}) \quad (1.18)$$

Defining the total mechanical energy as  $E = \frac{1}{\rho} P + \frac{1}{2} |\mathbf{u}|^2$  (sum of kinetic energy and energy due to total pressure). Taking a divergence of Eq.(1.18) and using the continuity equation gives:

$$\begin{aligned}\nabla^2 E &= \nabla \cdot (\mathbf{u} \times \boldsymbol{\omega}) \\ &= \boldsymbol{\omega} \cdot \boldsymbol{\omega} - \mathbf{u} \cdot (\nabla \times \boldsymbol{\omega})\end{aligned} \quad (1.19)$$

We express total mechanical energy as a mean and a deviation from mean as  $E = E_m + \varepsilon E_d$ , and  $\mathbf{u} = \mathbf{u}_m + \varepsilon \mathbf{u}_d$  and  $\boldsymbol{\omega} = \boldsymbol{\omega}_m + \varepsilon \boldsymbol{\omega}_d$ . Defining  $\Omega_d = \boldsymbol{\omega}_m \cdot \boldsymbol{\omega}_d$ , and subtracting the equation for mean flow from instantaneous flow, one gets the equation for ‘‘Disturbance Mechanical Energy’’ ( $E_d$ ) given as:

$$\nabla^2 E_d = \Omega_d + \varepsilon \boldsymbol{\omega}_d \cdot \boldsymbol{\omega}_d - \mathbf{u}_m \cdot (\nabla \times \boldsymbol{\omega}_d) - \mathbf{u}_d \cdot (\nabla \times \boldsymbol{\omega}_m) - \varepsilon \mathbf{u}_d \cdot (\nabla \times \boldsymbol{\omega}_d) \quad (1.20)$$

The positive (negative) value of RHS signify a sink (source) of the  $E_d$ . LHS of Eq.(1.19) can be written as:

$$\nabla^2 E = \nabla^2 \left( \frac{1}{\rho} P + \frac{1}{2} |\mathbf{u}|^2 \right) = 2Q + \nabla^2 \frac{1}{2} |\mathbf{u}|^2 \quad (1.21)$$

Where Eq.(1.3) was used. In case of a zero pressure gradient flow,  $\nabla^2 P = \nabla^2 P_d$  since mean pressure is a constant quantity. Using this we can rewrite LHS of Eq.(1.20) as

$$\nabla^2 E_d = 2Q + \frac{1}{2} \nabla^2 (|\mathbf{u}|^2 - |\mathbf{u}_m|^2) \quad (1.22)$$

This equation gives the relation between Q criteria and DME. Thus DME can be used for vortex identification. RHS of Eq.(1.20) being positive gives the regions of sink of disturbance mechanical energy in the flow, while the regions of negative RHS are sources of disturbance mechanical energy. This can also be used to visualize the flow due to presence of source and sink of disturbance mechanical energy.

# Chapter 2

## Methods

The flow analyzed in this thesis was simulated at HPCL, IITK [19]. A brief description of this is given in the next section.

### 2.1 Flow Details

The flow used for analysis is obtained by Direct Numerical Simulation (DNS) of a flow over a flat plate [19]. Velocity-vorticity formulation of Navier-Stokes equation as discussed in [17,18] is used for this simulation. The governing vorticity transport equation (VTE) in non-dimensionalised form is given by:

$$\frac{\partial \vec{\omega}}{\partial t} + \nabla \times (\vec{\omega} \times \vec{V} + \frac{1}{Re_L} \nabla \times \vec{\omega}) = 0 \quad (2.1)$$

where  $Re_L$  is the Reynolds number defined based on free-stream velocity and a representative length scale. For the current simulation,  $Re_L = 10^5$ . The vorticity field is obtained directly by solving the governing VTE, while the velocity field is obtained by solving the vector poisson equations  $\nabla^2 \vec{V} = -\nabla \times \vec{\omega}$  for  $u$ - and  $w$ -components while the  $v$ -component is calculated by integrating the continuity equation. Time integration is done by using an optimized, dispersion relation preserving three-stage Runge-Kutta scheme [18]. A staggered grid [20,21] is used, with velocity components evaluated at the face centers and the vorticity components evaluated at the edge centers, to minimize error in numerical diver-

gence of vorticity.

The domain of computation, shown in Fig:(2.1) stretches from  $-0.05L \leq x \leq 50L$  in  $x$ -direction,  $0 \leq y \leq L$  in  $y$ -direction and  $-0.25L \leq z \leq 0.25L$  in  $z$ -direction. A uniform flow with free stream non-dimensional velocity  $u = 1$  is supplied at the inflow. At the outflow, sommerfeld boundary conditions as detailed in [18] is used. A periodic boundary condition is used along the span-wise( $z$ ) direction. At the top of domain,  $u = 1, w = 0$  and  $v$  is calculated from continuity equation. The boundary condition for vorticity at the top of domain is  $\omega_x = \omega_y = 0$  and  $\frac{\partial \omega_y}{\partial y} = 0$ . At the bottom of domain, before the leading edge,  $\frac{\partial u}{\partial y} = \frac{\partial w}{\partial y} = \frac{\partial \omega_y}{\partial y} = 0$  and  $v = \omega_z = \omega_x = 0$ .

The number of points used in  $x$ -,  $y$ - and  $z$ -directions are  $2501 \times 351 \times 49$ , with grid points concentrated near the leading edge of flat plate in  $x$ -direction and near the wall in  $y$ -direction. The equilibrium flow obtained is perturbed by an excitation strip at the wall with excitation given by  $v(x, y = 0, z) = A(t)A(x, z)$ . Here  $A(t) = \sin(10t)(1 + \text{erf}(\frac{t-4}{0.25066}))$  where the error function ( $\text{erf}(x)$ ) is used to start the exciter non-impulsively, and  $A(x, z) = 0.005(1 + \cos 2\pi x_{ex})\sin(8\pi z)$  with  $x_{ex} = 11.111 \times (x - 1.5)$ . The exciter strip has a stream-wise extent of  $1.455 \leq x \leq 1.545$ . The non-dimensional frequency of the time harmonic excitation is given by  $F = \frac{\omega}{Re_L} = 1 \times 10^{-4}$ .

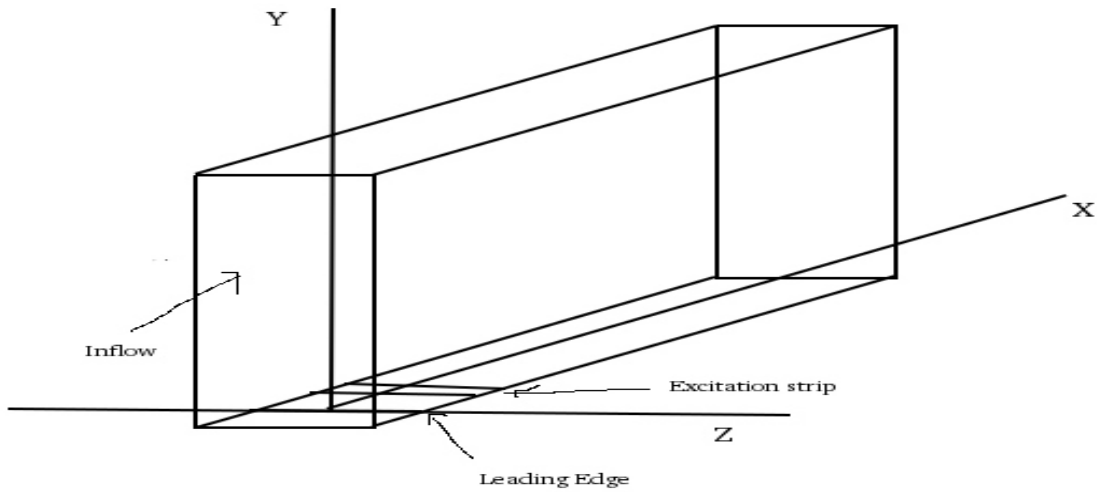


Figure 2.1: Computational domain of the flat plate flow

## 2.2 Calculation of different criteria

### 2.2.1 Vorticity

Vorticity field is obtained directly by solving the governing equation in the velocity-vorticity formulation and is used as-is.

### 2.2.2 $\lambda_2$ -criteria and $Q$ -criteria

The velocity derivatives are calculated at the staggered locations using a central difference scheme, and interpolated to grid points. These derivatives are used to generate the velocity gradient tensor at the grid points. The velocity gradient tensor is then broken into its symmetric ( $\mathbf{S}$ ) and antisymmetric ( $\mathbf{\Omega}$ ) parts.

To calculate  $\lambda_2$ -criteria, we find the eigenvalues of  $(\mathbf{\Omega}^2 + \mathbf{S}^2)$  using the lapack subroutine 'dsyev', which gives the eigenvalues in descending order, and select the second eigenvalue. For  $Q$ -criteria calculation, we add these eigenvalues and store them (Eq.(1.8)).

### 2.2.3 Rortex

Rortex is calculated by doing a schur decomposition of velocity gradient tensor using lapack subroutine 'dges' to obtain the 'M'-matrix and the velocity gradient tensor in new coordinates in Eq.(1.9). Eq.(1.12) and Eq.(1.11) are used to find the  $g_z|_{\theta}$  and its minimum is the value of rortex. The direction of rortex is found by using Eq.(1.10)

### 2.2.4 DETE

To calculate DETE, the vorticity field is first interpolated from the staggered grid to the grid points. The RHS of vorticity transport equation Eq.(1.15) is then calculated for the base flow (flow before excitation was provided) and the instantaneous flow. The RHS of Eq.(1.15) for the base flow is subtracted from that of instantaneous flow to obtain the DETE



value. The value of disturbance enstrophy ( $\Omega_d$ ) is obtained by subtracting the vorticity of base flow from the vorticity of instantaneous flow.

As we need to identify the regions where disturbances are amplified, we find the regions with both  $\Omega_d$  and DETE positive by:

$$DETE(+ve) = \frac{(\Omega_d + |\Omega_d|)(DETE + |DETE|)}{(\Omega_d + |\Omega_d|) + \varepsilon} \quad (2.2)$$

and regions with both  $\Omega_d$  and DETE negative by:

$$DETE(-ve) = \frac{(\Omega_d - |\Omega_d|)(DETE - |DETE|)}{(\Omega_d - |\Omega_d|) + \varepsilon} \quad (2.3)$$

here  $\varepsilon$  is a small number =  $10^{-15}$

### 2.2.5 DME

To calculate DME, the RHS of Eq.(1.19) is evaluated for both the instantaneous flow and base flow. The value base flow is then subtracted from that of instantaneous flow to get the value of Disturbance Mechanical Energy at the grid point.

## 2.3 Correlation Methodology

The isosurface values of different criteria plotted in figures are based on a statistical correlation between the criteria ( $|\vec{\omega}|, \lambda_2, Q, DME, Rortex$ ) vs DETE. We use DETE rather than vorticity as the basis for this method as it is known that vorticity is not a good measure to identify vortices in shear flows due to presence of a large vorticity bank in the shear region even in the absence of vortices. Another advantage of choosing DETE as the basis is that this method is derived directly from vorticity-transport equation without any simplifications and contains all the terms of the equation, unlike the other criteria in which the straining and viscous terms are either neglected or do not appear due to the definition. Also, due to the absence of pressure term in DETE equation, the straining and viscous terms do not cause any anomalous effects, and hence need not be neglected to identify coherent

structures.

The correlation methodology is based on grid search, i.e. we find the grid-points DETE attains a value of  $a \pm 5\%$  ( $a$  is the basis value of DETE), and check for the values of other criteria ( $|\vec{\omega}|, \lambda_2, Q, \text{DME}, \text{Rortex}$ ) at these grid-points. This is repeated for each required value of DETE. In order to perform this search, a sub-region of the computed domain is identified. This sub-region is selected to lie in the region of transitional/turbulent flow where coherent structures will be present. Mean and standard-deviation of each criteria for a particular value of DETE is computed and used as the correlated value of the other criteria.

# Chapter 3

## Results and Discussions

### 3.1 Comparison of different criteria

We show a visual comparison between DETE, DME,  $\lambda_2$ -criteria,  $Q$ -criteria and Rortex for  $t=25.3$  and  $t=29.3$  in Figs:(5.1, 5.2). Here, DETE(positive/negative) is defined as region where both DETE and  $\Omega_d$  are positive/negative (Eq.2.2, Eq.2.3). These regions correspond with a growth of disturbance enstrophy in time.

It is seen that the large scale structures identified by each criteria are similar and of the same size for  $t = 29.3$ , which is not the case for  $t = 25.3$ . At  $t = 25.3$ , the structures in all the criteria are identified in the same region, but DETE and DME identify flatter structures compared to other criteria. It is also observed from Fig:(5.3 a) that the vorticity field at this time is smooth and has not experienced non-linear effects. Thus, DETE and DME are seen to be able to differentiate between flow before and after the onset of non-linear growth of disturbance by the quality of the structures. After the onset of non-linear growth, all criteria provide similar results as seen in Fig:(5.2).

It is also observed that DME does not cover the entire coherent structure with a single isosurface, rather both positive and negative DME together form the observed structure. DETE as well has a combination of both its positive and negative contributions inside the boundary layer, but is dominated by positive contribution outside the boundary layer. This domination of positive contribution outside of the boundary layer is due to the fact that in

the base flow, regions outside the boundary layer had no enstrophy thus any addition of enstrophy to this region will be a positive contribution to disturbance enstrophy. The presence of structures outside of boundary layer is caused by the non-linear growth of disturbance, as in Eq.(1.17) the linearized  $\Omega_d$  given by  $\omega_m \cdot \omega_d$  would be  $\approx 0$  in this region, but the total disturbance enstrophy ( $= \Omega - \Omega_m$ ) is a non-zero value with considerable magnitude.

A comparison of structures in the region closer to the exciter in Figs:(5.1, 5.2) shows another difference.  $Q-$ ,  $\lambda_2-$  and Rortex (c,d,e in the respective figures) identify structures at the leading edge, which are absent from DETE and DME structures. These structures are not vortices, and are a result of including the leading edge in the flow domain, which creates a stagnation line resulting in high vorticity at the leading edge.

## 3.2 Evolution of the flow

Figures:(5.3 to 5.8) show the time evolution of enstrophy, DETE and wall-normal velocity at the anti-nodal location  $z = 0.1875$ . Figures:(5.9 to 5.11) show the same at the anti-nodal location  $z = 0.0625$ . It is observed that undulations in the enstrophy structures appear around  $t = 25.3$  at  $12 < x < 13$  for  $z = 0.1875$ , while they are already present at  $12 < x < 13$  before  $t = 25.1$ . The location of undulation corresponds with region of positive  $v$ -velocity at  $z = 0.1875$  and with negative  $v$ -velocity at  $z = 0.0625$ . It is also observed that this undulation appears when the overlap of DETE and enstrophy has lost its symmetry. The undulation starts at all spanwise locations in the same streamwise strip, and on the second enstrophy spike. These undulations carry the signature of how the flow was excited, namely of suction and blowing. Antinodal locations ( $z = -0.0625, z = 0.1875$ ) show similar undulations caused by ejections, while those at ( $z = -0.1875, z = 0.0625$ ) are caused by sweeps in the region. This memory of exciter cannot be distinguishably seen at later times due to an increase in number of small scale interacting structures in the turbulent spot.

Another observation is that alternating of DETE(-ve) and DETE(+ve) results in clubbing of excited wavelets and a conversion from an alternating structure to a linear structure. It is seen that the exciter results in many wavelets of enstrophy and DETE (evident from the flow near the exciter), while the flow at locations  $x > 11$  appears to have two spikes of enstrophy and another one that is still growing. This growth of spike also can be explained

as DETE(-ve) results in reduction of enstrophy from the mean while DETE(+ve) results in an increase from the mean. The alternation of these gives rise to these spikes, which are formed by a combination of various small wavelets of enstrophy generated at the exciter.

### 3.3 Correlation of criteria

While correlating the different criteria at a given time, we change DETE(+ve) values and correlate the other criteria with respect to each value of DETE(+ve) chosen. The resulting histograms for time  $t = 27.1$  and DETE(+ve)= 100 are shown in Fig:(5.12,5.13). It can be observed that histograms of correlation of DETE with  $Q$ - and  $\lambda_2$ -criteria have a small number of large outliers. Fig:(5.14) shows the effect of including and excluding these outliers on the mean and standard deviation. It is observed that there is a major difference between the statistics with and without outliers for  $\lambda_2$ - and  $Q$ -criteria while the same for DME and  $|\vec{\omega}|$  is not much. Due to this, the statistics without outlier is used in all subsequent correlation plots. Figs:(5.15-5.25) show the correlation of all criteria with respect to DETE for times  $t=25.1$  to  $t=29.3$ . It can be observed from these figures that correlation of  $|\vec{\omega}|$  vs DETE appear to be similar at all times considered, and follow a logarithmic profile, as plotted in Fig:(5.26) for  $27.1 \leq t \leq 29.3$  to reduce clutter. Here DETE is fitted to exponential of vorticity as the plotting software does not support fitting of data to a logarithmic profile. This gives an equation of correlation of the form:

$$DETE = exp(\alpha(t)|\vec{\omega}| + \beta(t)) \quad (3.1)$$

the plot of  $\alpha(t)$  and  $\beta(t)$  with respect to time is as shown in Fig:(5.27). In order to find the scaling factors, we fit various curves to  $\alpha(t)$  and  $\beta(t)$  given by  $a(t)$  and  $b(t)$  respectively, and scale the data points as  $DETE \rightarrow \frac{DETE}{e^{b(t)}}$  and  $|\vec{\omega}| \rightarrow \frac{a(t)|\vec{\omega}|}{a_0}$ . We attempt to find the fit ( $a(t)$  and  $b(t)$ ) such that the difference between the exponential fits (like Eq.(3.1)) of scaled variables in time is minimized. This results in a quadratic fit  $a(t)$  and a sine function fit for  $b(t)$  given by

$$a(t) = 2.585 - 0.2064 * t + 0.004385 * t^2 \quad (3.2)$$

$$b(t) = 0.5072sin(1.094 * t - 1.193) + 0.1414 \quad (3.3)$$

the resulting scaled variable fit is shown in Fig:(30) where (a) shows the result for each

time separately, while (b) shows the same for all times together. It is observed that the deviation of fit in the newly scaled variables is considerably less than that in the original variables.

# Chapter 4

## Summary and Conclusion

During the course of this thesis, we attempted to compare DETE and DME with some popular vortex identification criteria. It was observed that DME and DETE are able to differentiate between the stable and unstable regions in the flow better than the other criteria. It is also seen that the structures identified by  $\lambda_2$ - and  $Q$ - criteria need not all be vortices. This is a point that is also emphasized in some discussions on coherent structures within the research community. An attempt was made to explain the evolution of flow using DETE, during which it was hinted that the initiation of undulations in enstrophy can be a signature of the exciter, though the entire memory of the exciter is not present in the flow, as alternating regions of DETE(+ve) and DETE(-ve) result in a clubbing of different wavelets of disturbance generated by the exciter.

It was noted that DETE, DME and Rortex accord a physical meaning to the identified structures while the commonly used  $\lambda_2$ - and  $Q$ - criteria are only mathematical constructs without any physical meaning. In an attempt to give a physical meaning to these criteria, a correlation was attempted with respect to DETE, and a representative number showing the value of these criteria for a given value of DETE was obtained. This attempt showed that the correlation between these criteria and DETE is not good standard deviation obtained was high.

While correlating different criteria with DETE, it was observed that the correlation of DETE(+ve) with  $|\vec{\omega}|$  follows a similar profile at each time considered. A scaling factor for these criteria was identified. This scaling of DETE(+ve) with vorticity can be extended for

longer durations, and help create a simplified model to track the variation of vorticity with time.



# **Chapter 5**

## **Figures**

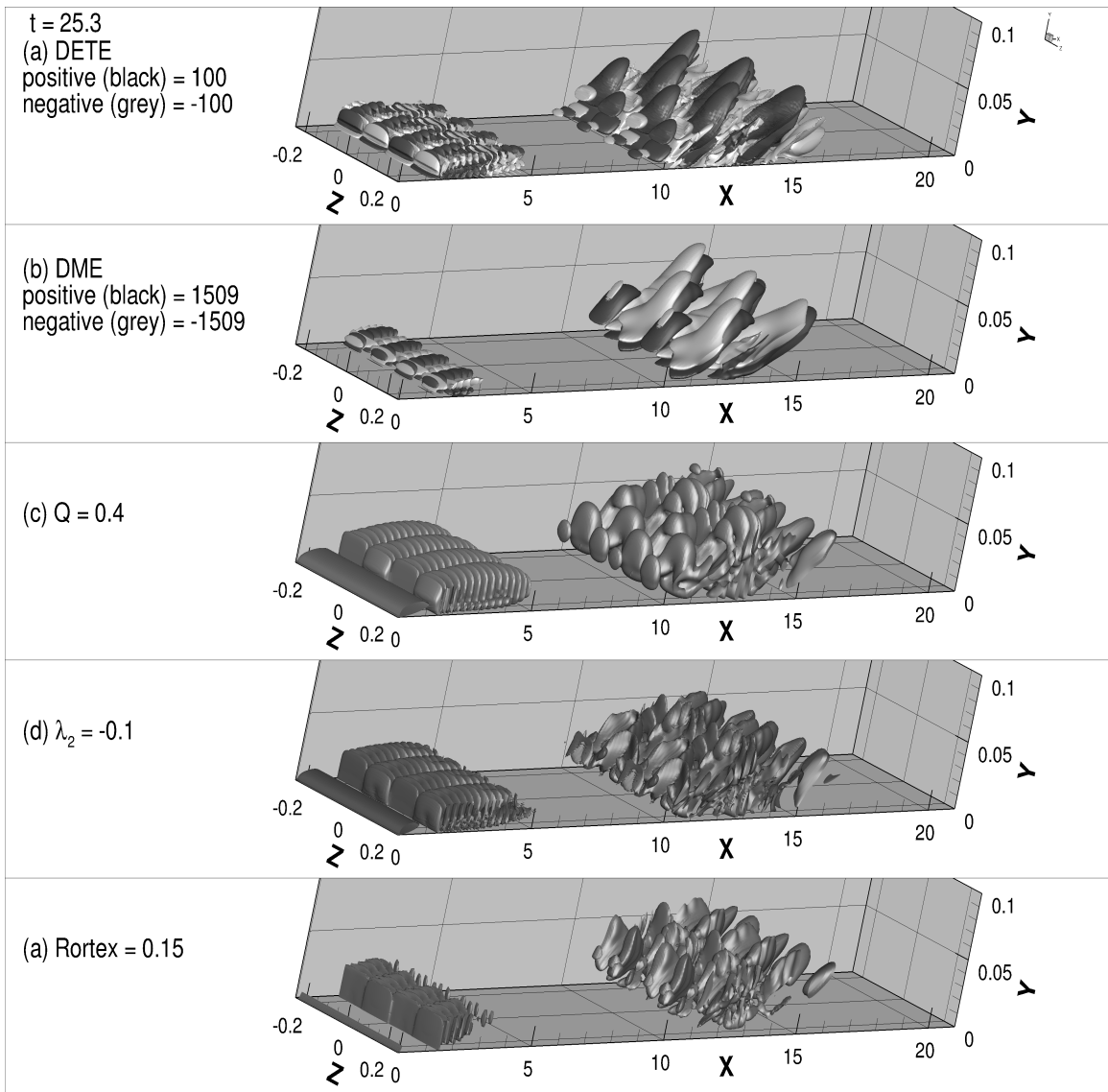


Figure 5.1: comparison between various criteria for  $t = 25.3$

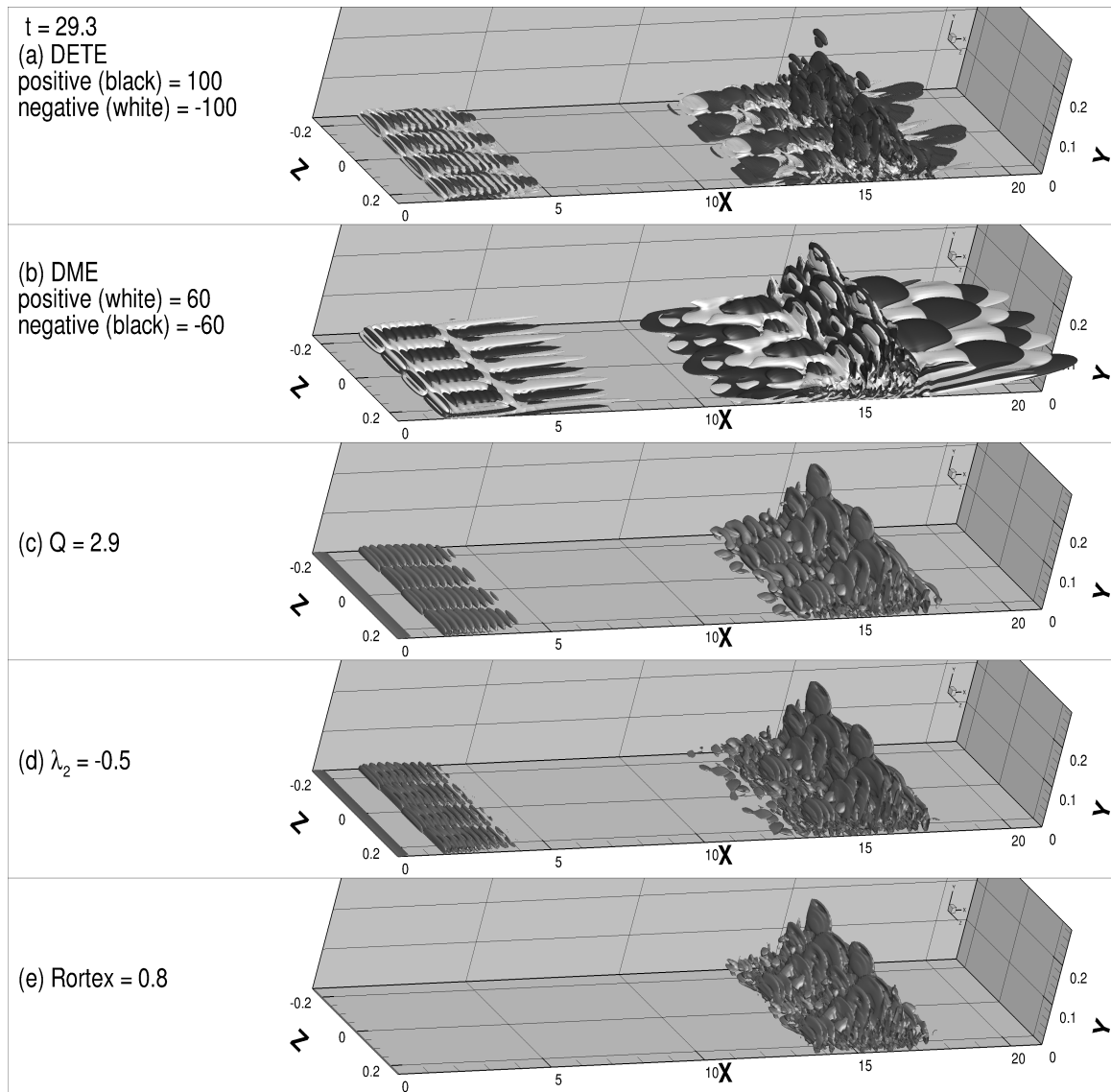


Figure 5.2: comparison between various criteria for  $t = 29.3$

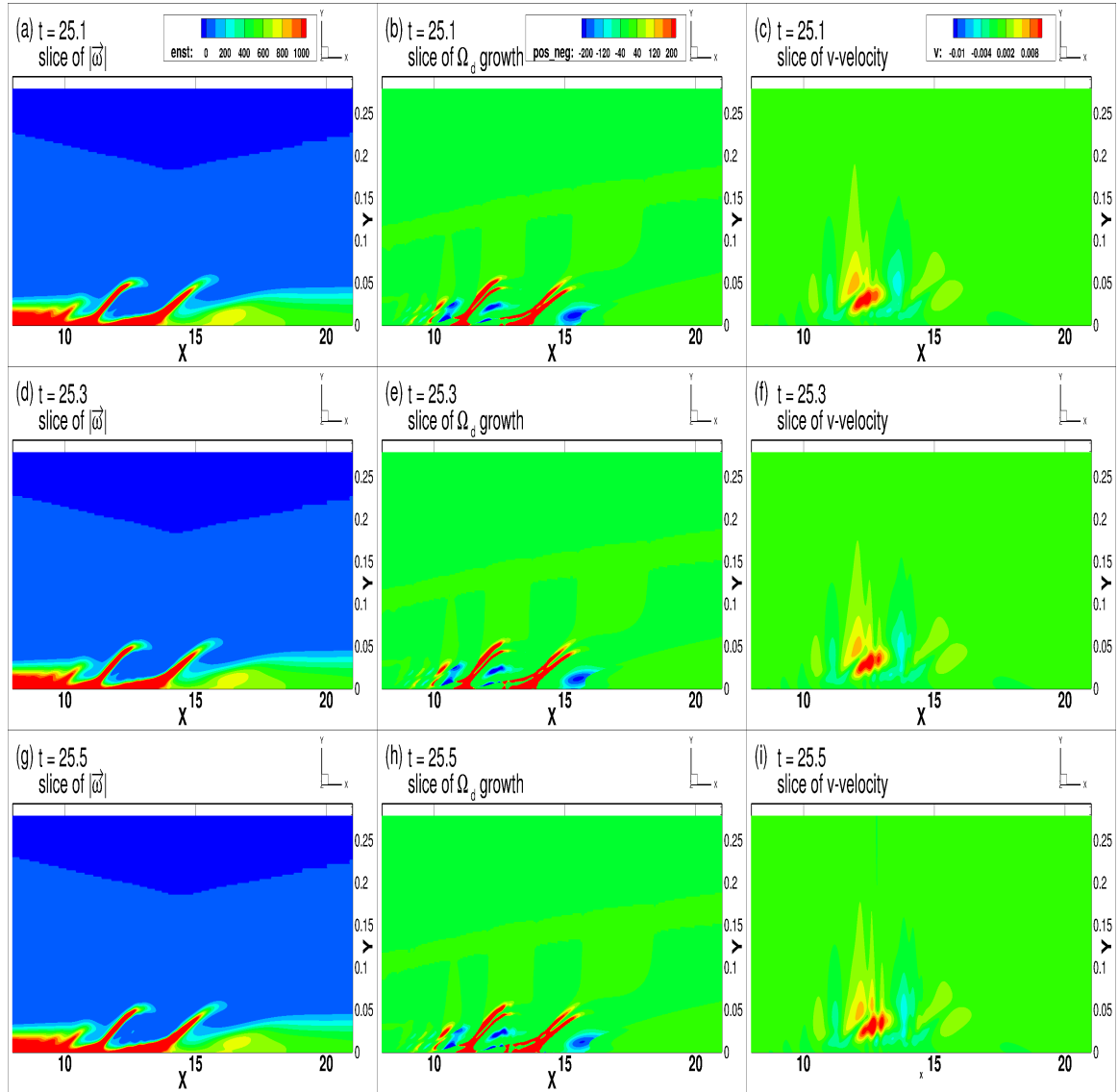


Figure 5.3: Slices of entrophy, DETE and  $v$ -velocity at different times at  $z = 0.1875$  (a,b,c) at  $t = 25.1$ , (d,e,f) at  $t = 25.3$ , (g,h,i) at  $t = 25.5$

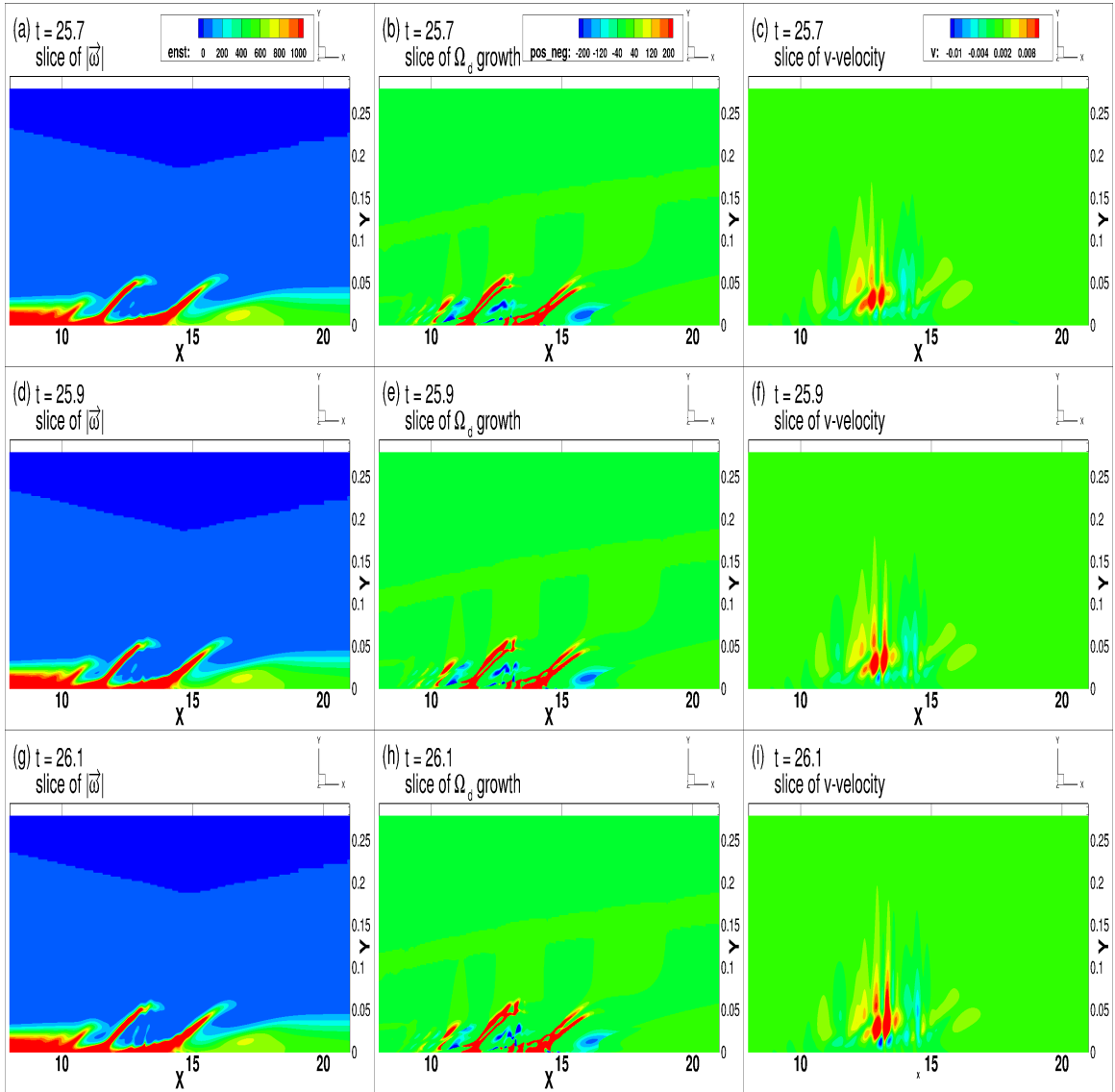


Figure 5.4: Slices of entrophy, DE TE and v-velocity at different times at  $z = 0.1875$  (a,b,c) at  $t = 25.7$ , (d,e,f) at  $t = 25.9$ , (g,h,i) at  $t = 26.1$

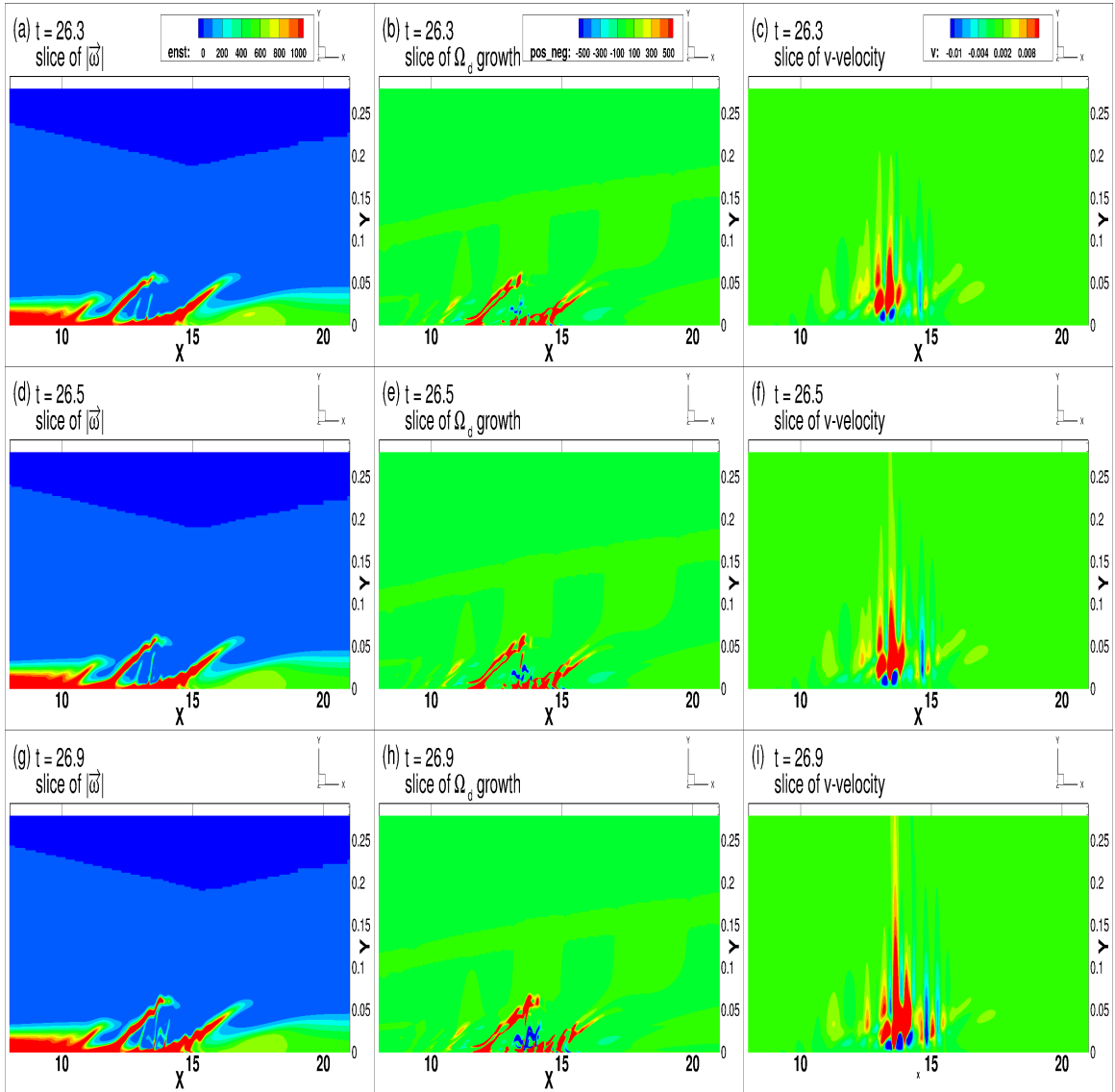


Figure 5.5: Slices of entrophy, DE TE and  $v$ -velocity at different times at  $z = 0.1875$  (a,b,c) at  $t = 26.3$ , (d,e,f) at  $t = 26.5$ , (g,h,i) at  $t = 26.9$

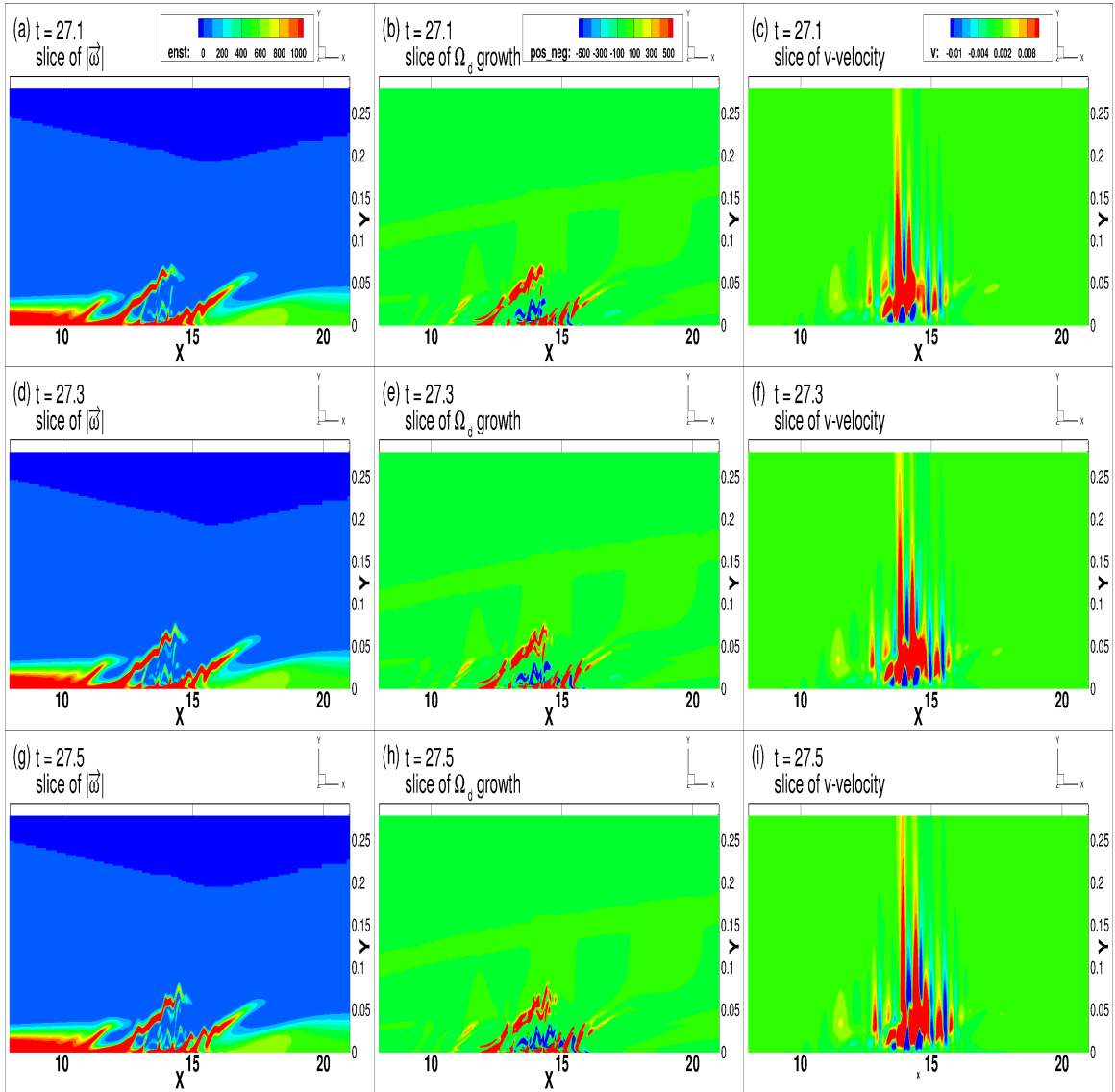


Figure 5.6: Slices of enstrophy, DE TE and  $v$ -velocity at different times at  $z = 0.1875$  (a,b,c) at  $t = 27.1$ , (d,e,f) at  $t = 27.3$ , (g,h,i) at  $t = 27.5$

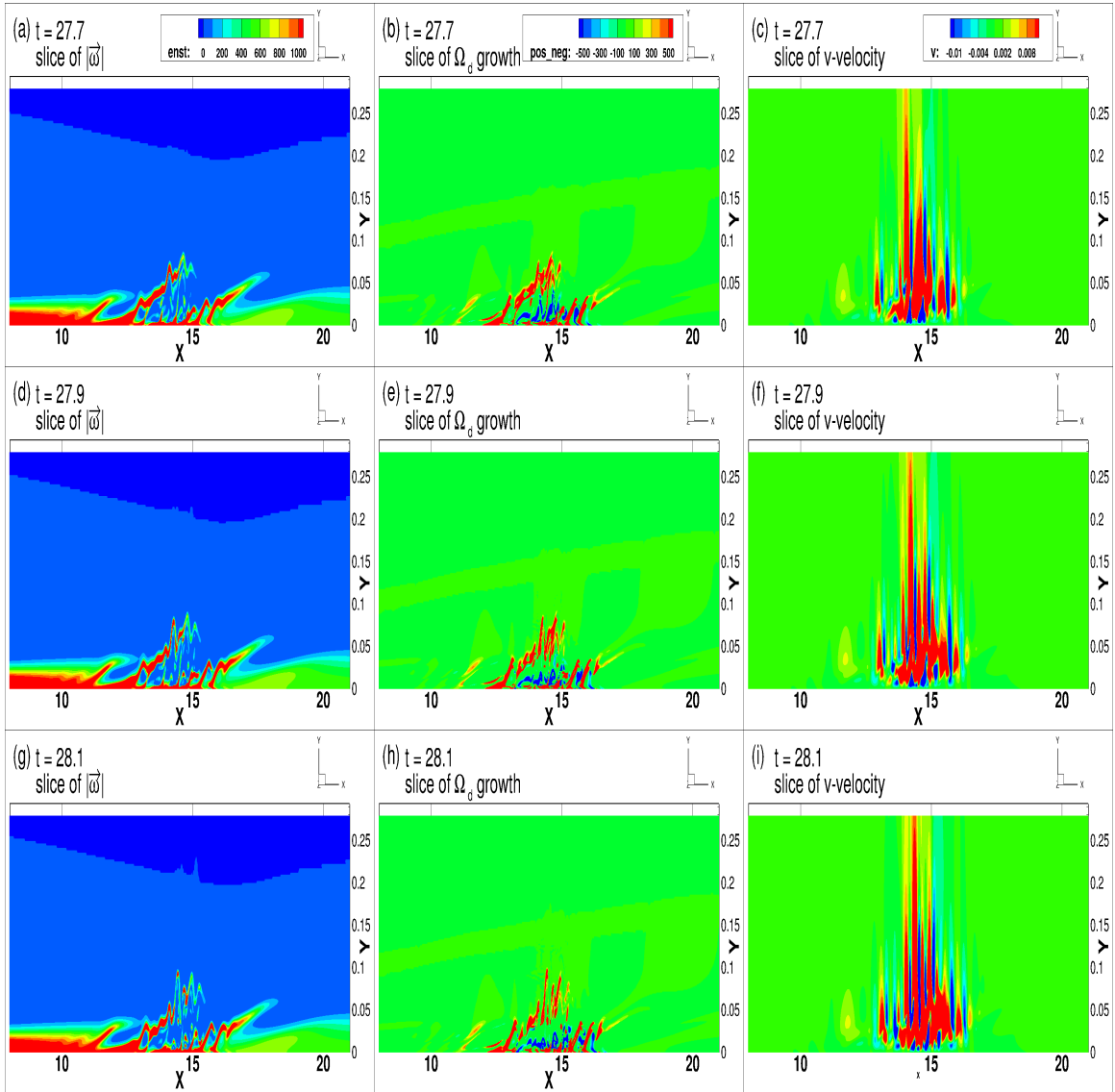


Figure 5.7: Slices of enstrophy, DE TE and v-velocity at different times at  $z = 0.1875$  (a,b,c) at  $t = 27.7$ , (d,e,f) at  $t = 27.9$ , (g,h,i) at  $t = 28.1$



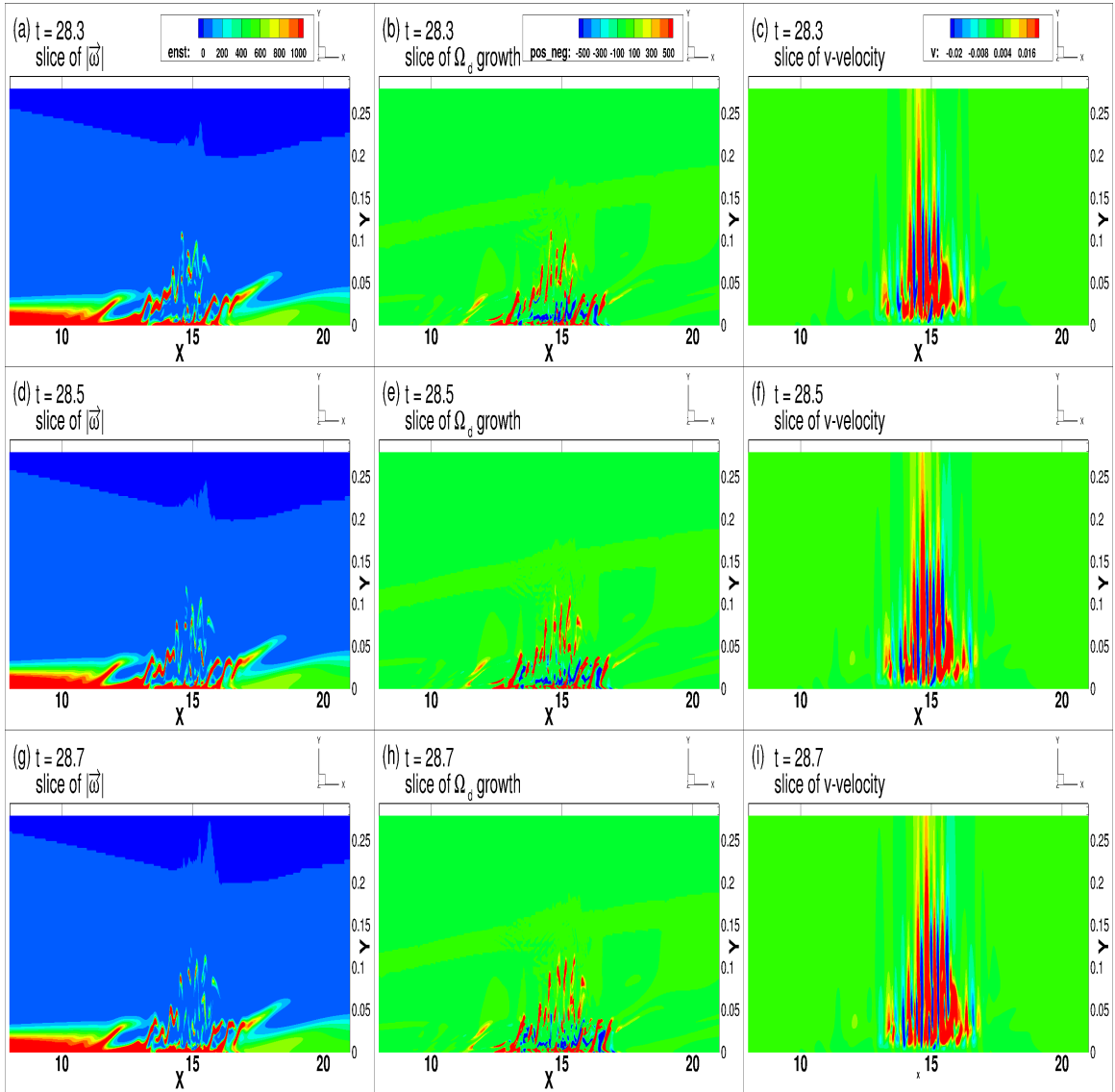


Figure 5.8: Slices of entrophy, DE TE and  $v$ -velocity at different times at  $z = 0.1875$  (a,b,c) at  $t = 28.3$ , (d,e,f) at  $t = 28.5$ , (g,h,i) at  $t = 28.7$

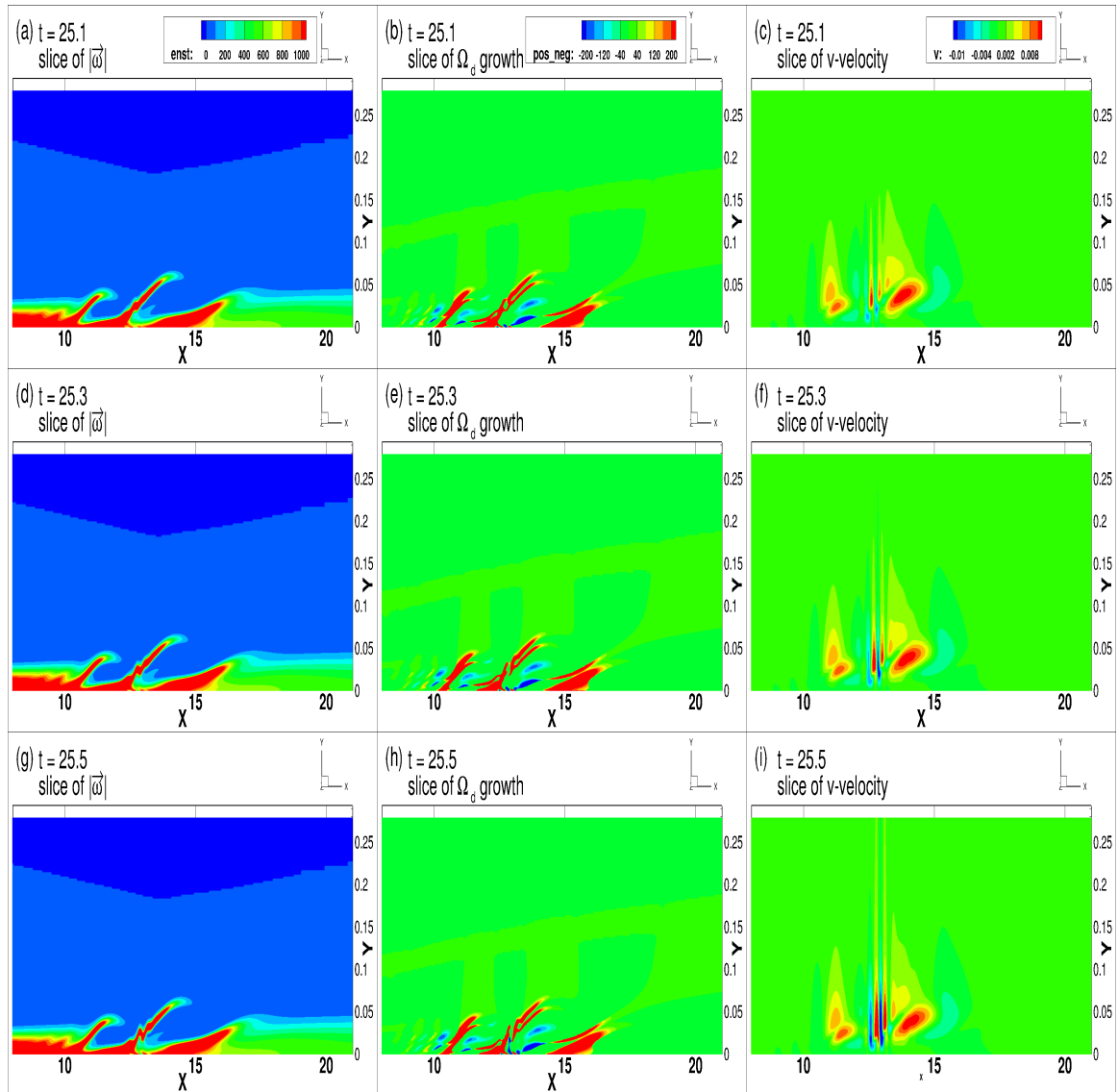


Figure 5.9: Slices of entrophy, DE TE and  $v$ -velocity at different times at  $z = 0.0625$  (a,b,c) at  $t = 25.1$ , (d,e,f) at  $t = 25.3$ , (g,h,i) at  $t = 25.5$

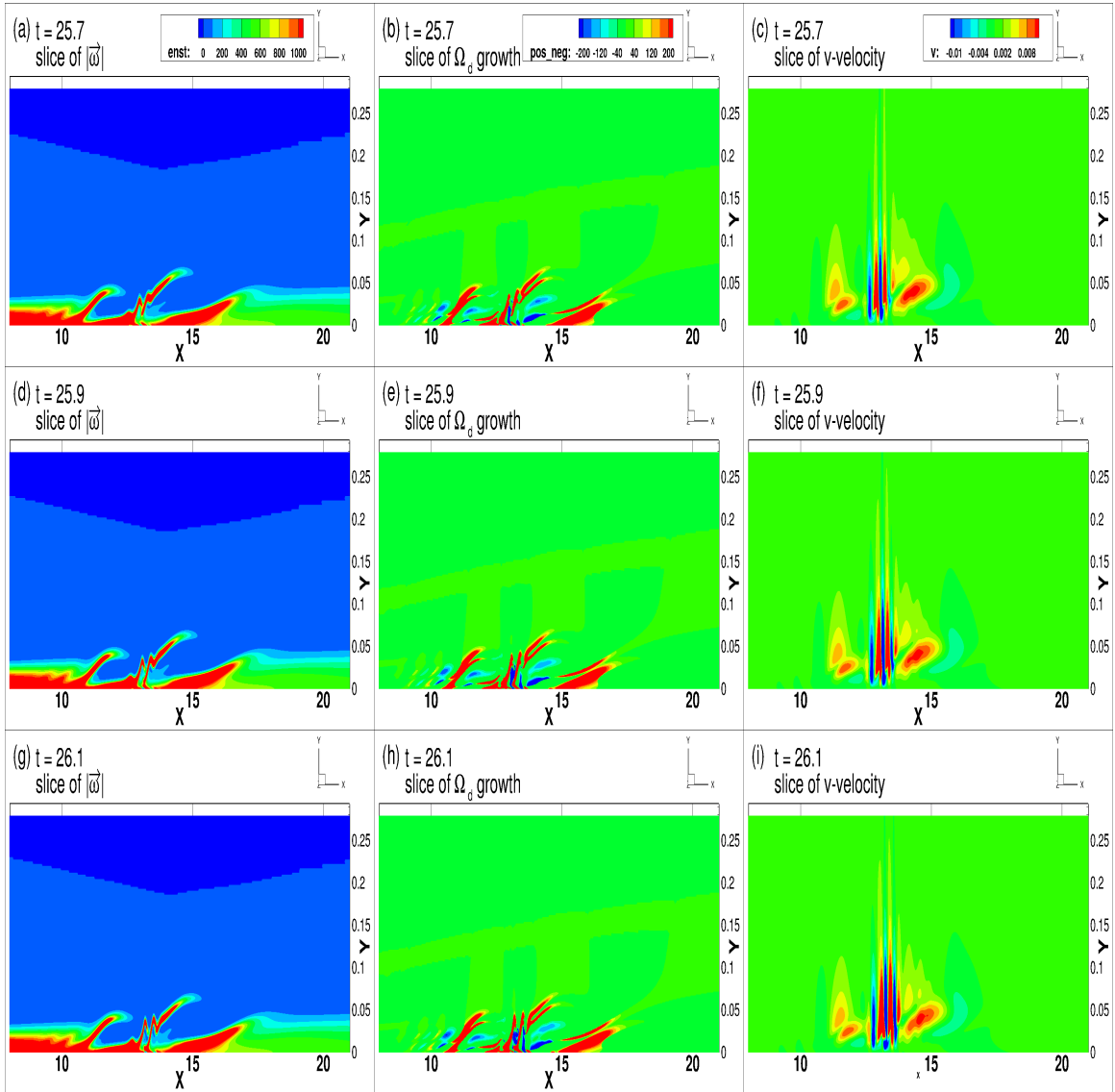


Figure 5.10: Slices of entrophy, DE TE and  $v$ -velocity at different times at  $z = 0.0625$  (a,b,c) at  $t = 25.7$ , (d,e,f) at  $t = 25.9$ , (g,h,i) at  $t = 26.1$

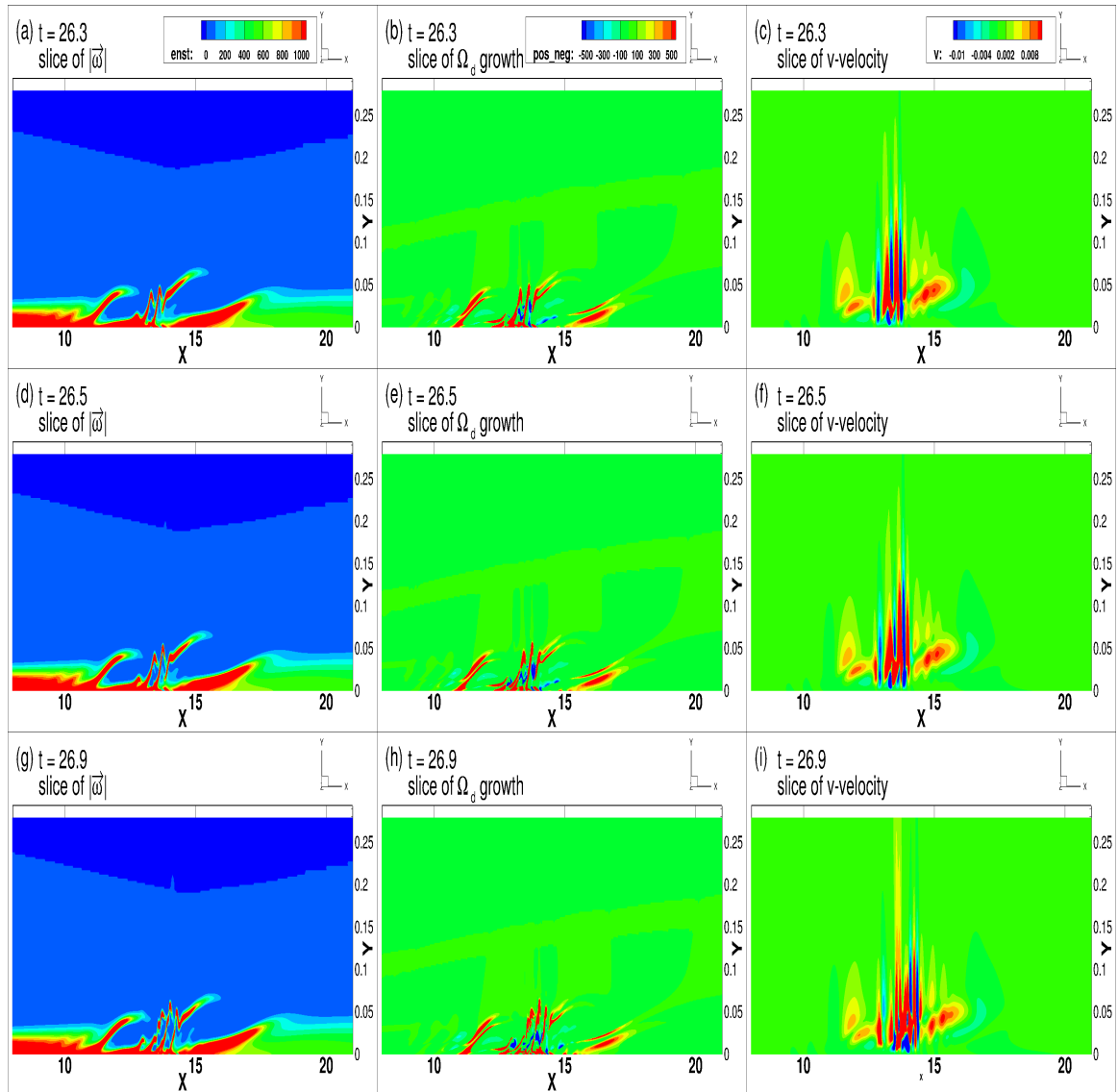


Figure 5.11: Slices of entrophy, DE TE and  $v$ -velocity at different times at  $z = 0.0625$  (a,b,c) at  $t = 26.3$ , (d,e,f) at  $t = 26.5$ , (g,h,i) at  $t = 26.9$

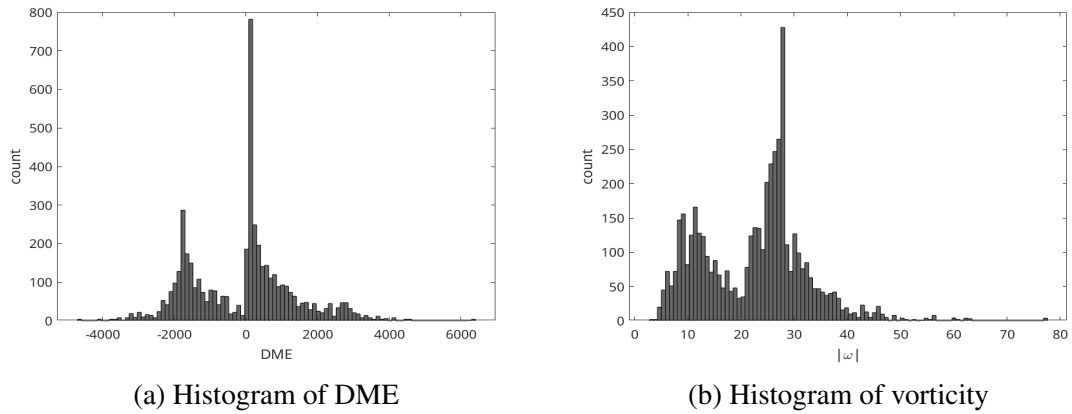


Figure 5.12: Histogram of DME and Vorticity for  $DETE = 100 \pm 5$  at  $t = 27.1$

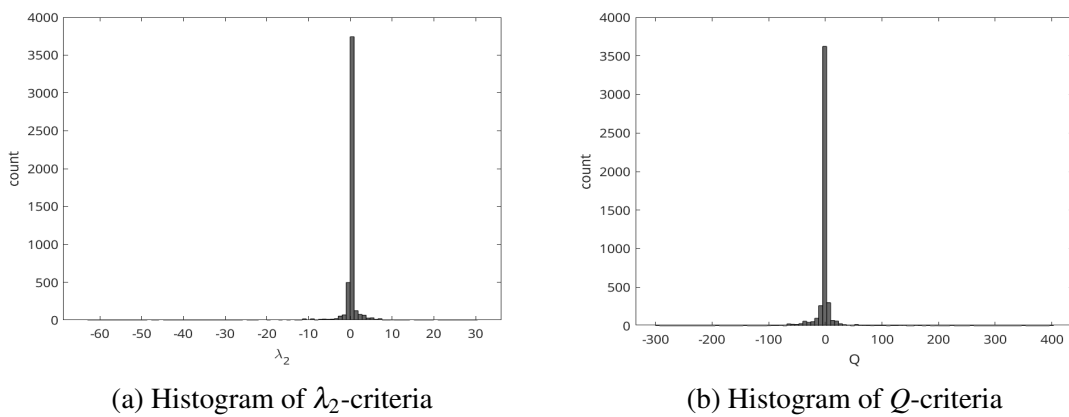


Figure 5.13: Histogram of  $\lambda_2$ - and  $Q$ - criteria for  $DETE = 100 \pm 5$  at  $t = 27.1$

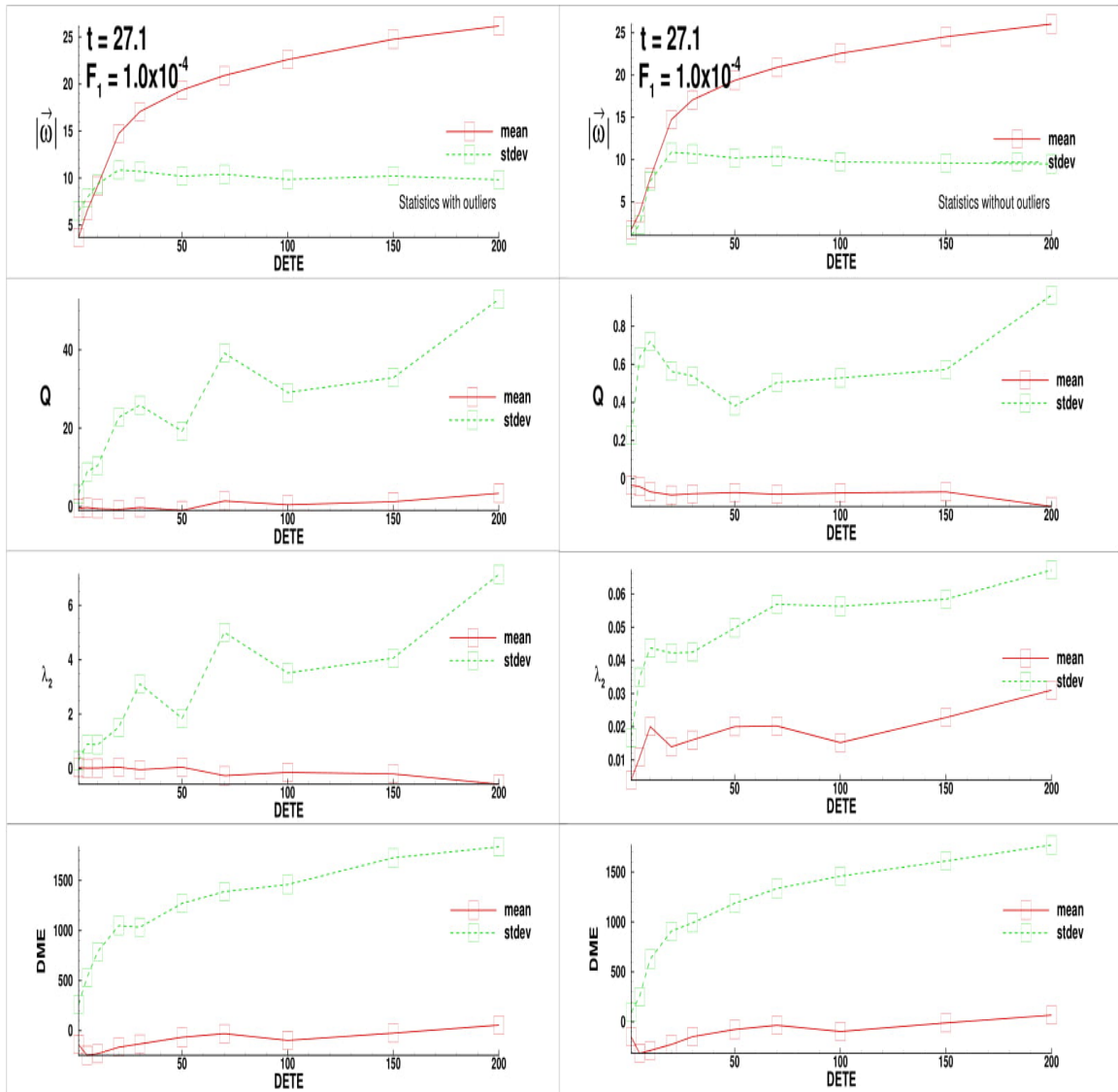


Figure 5.14: correlation of various criteria w.r.t DETE at  $t = 27.1$

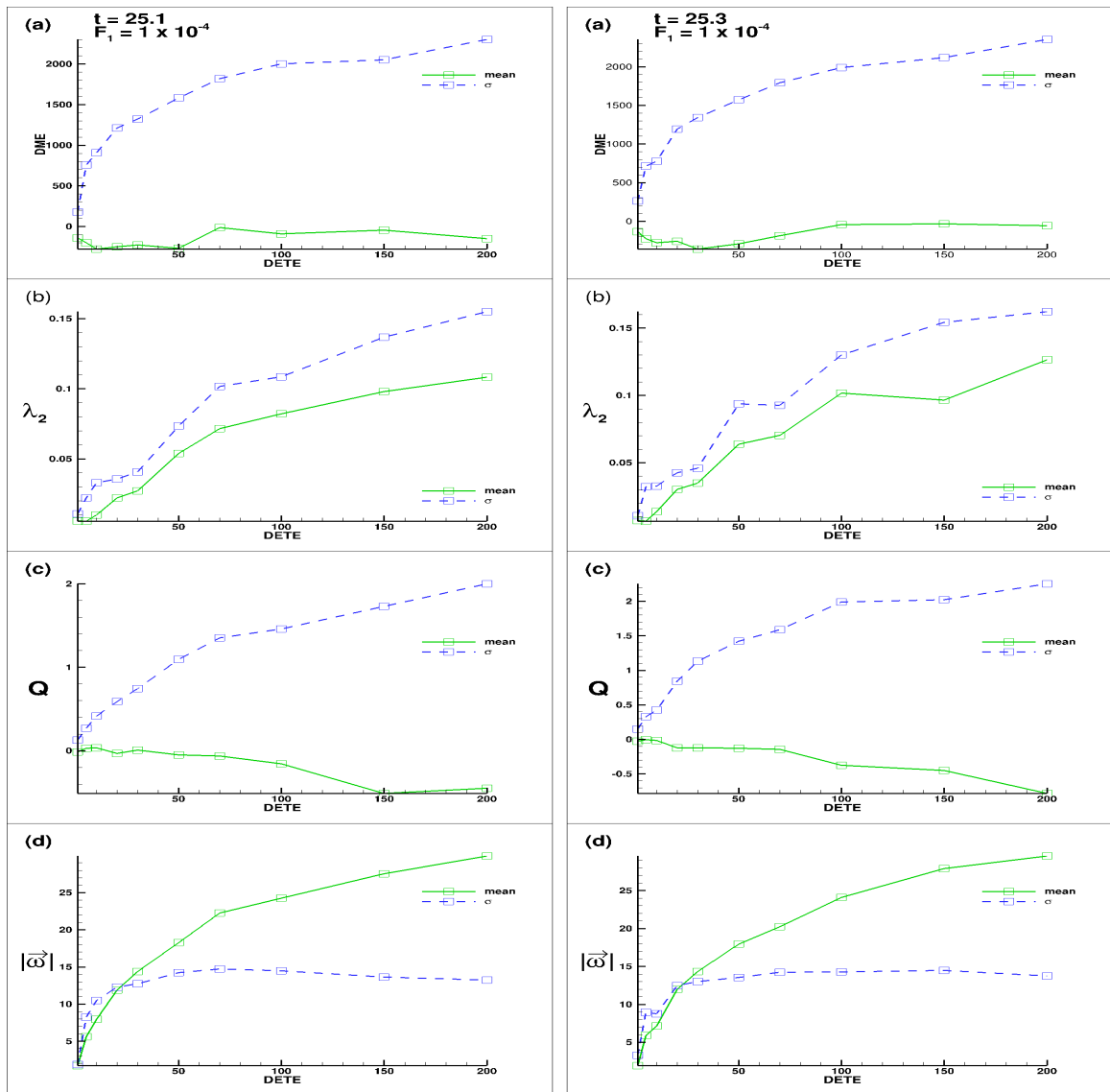


Figure 5.15: correlation of various criteria w.r.t DE TE

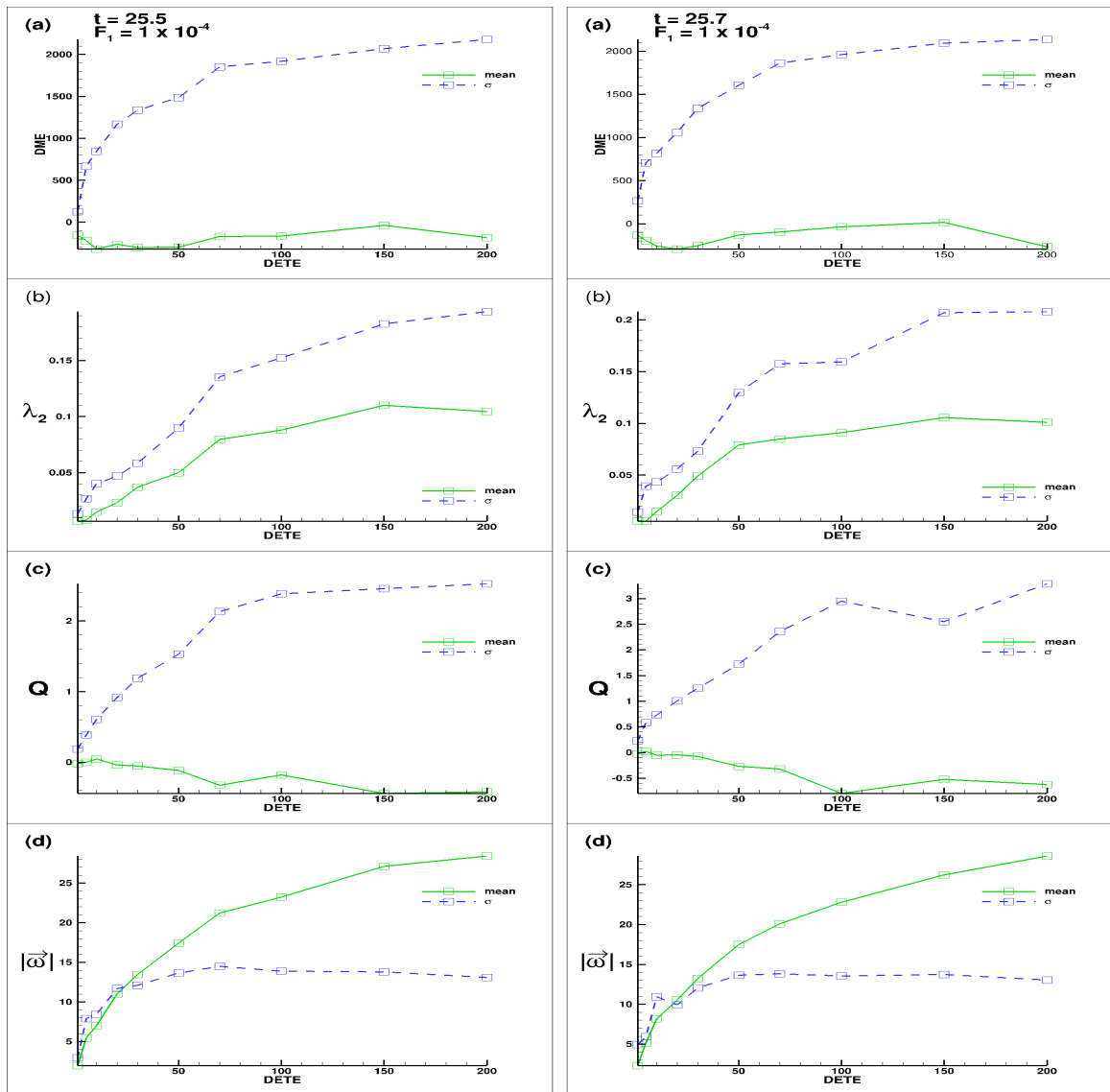


Figure 5.16: correlation of various criteria w.r.t DE TE



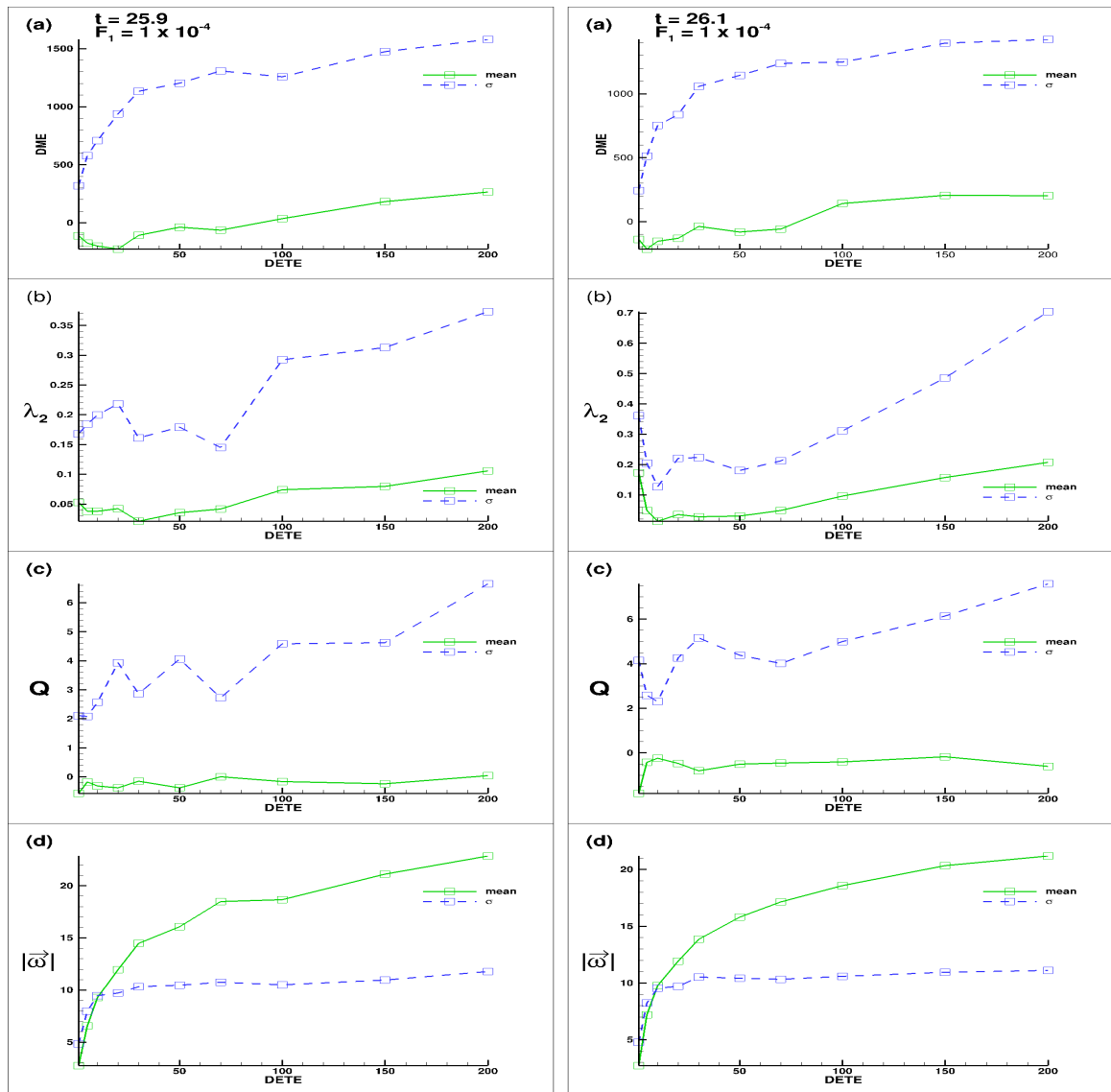


Figure 5.17: correlation of various criteria w.r.t DE TE

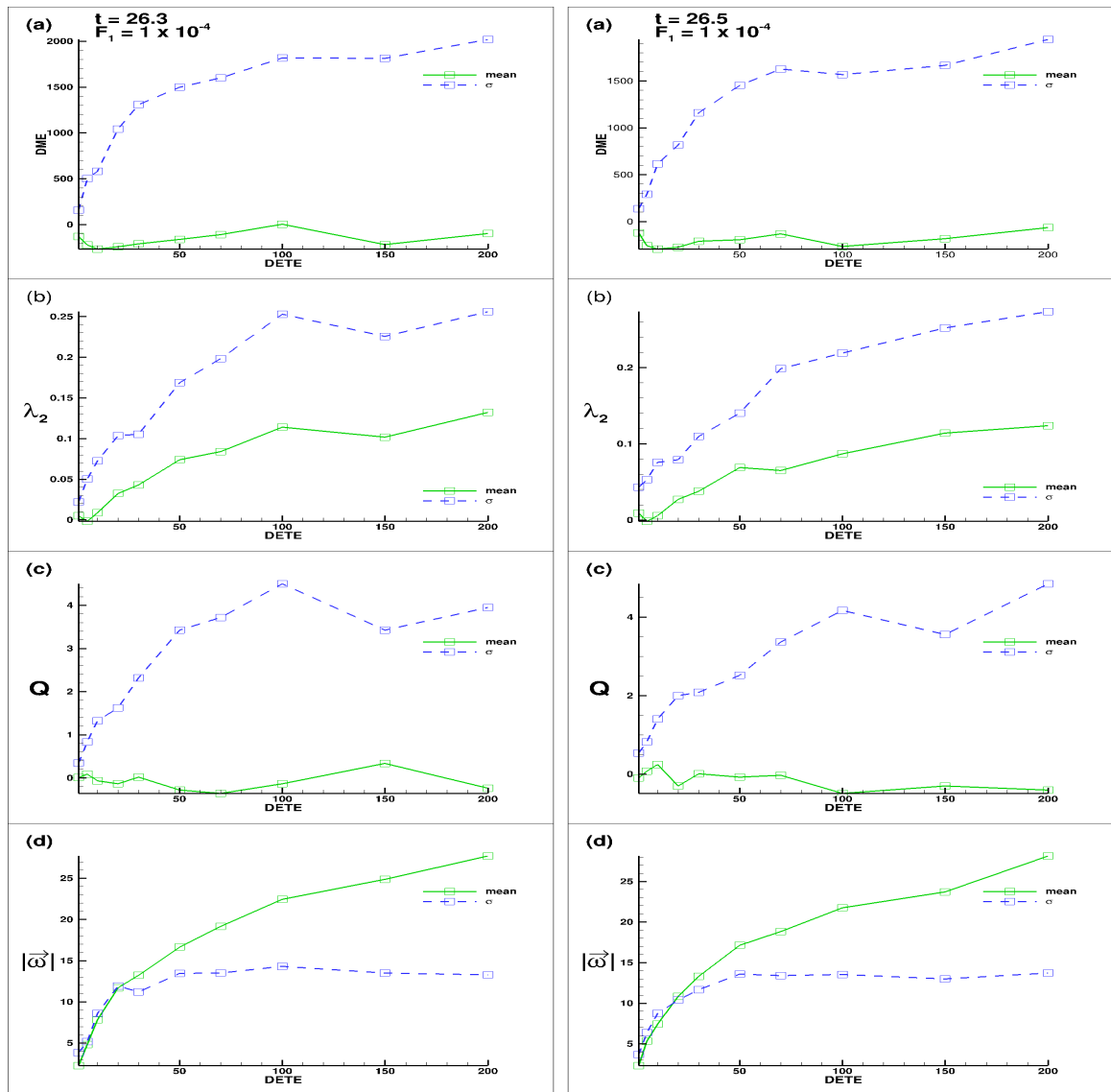


Figure 5.18: correlation of various criteria w.r.t DE TE

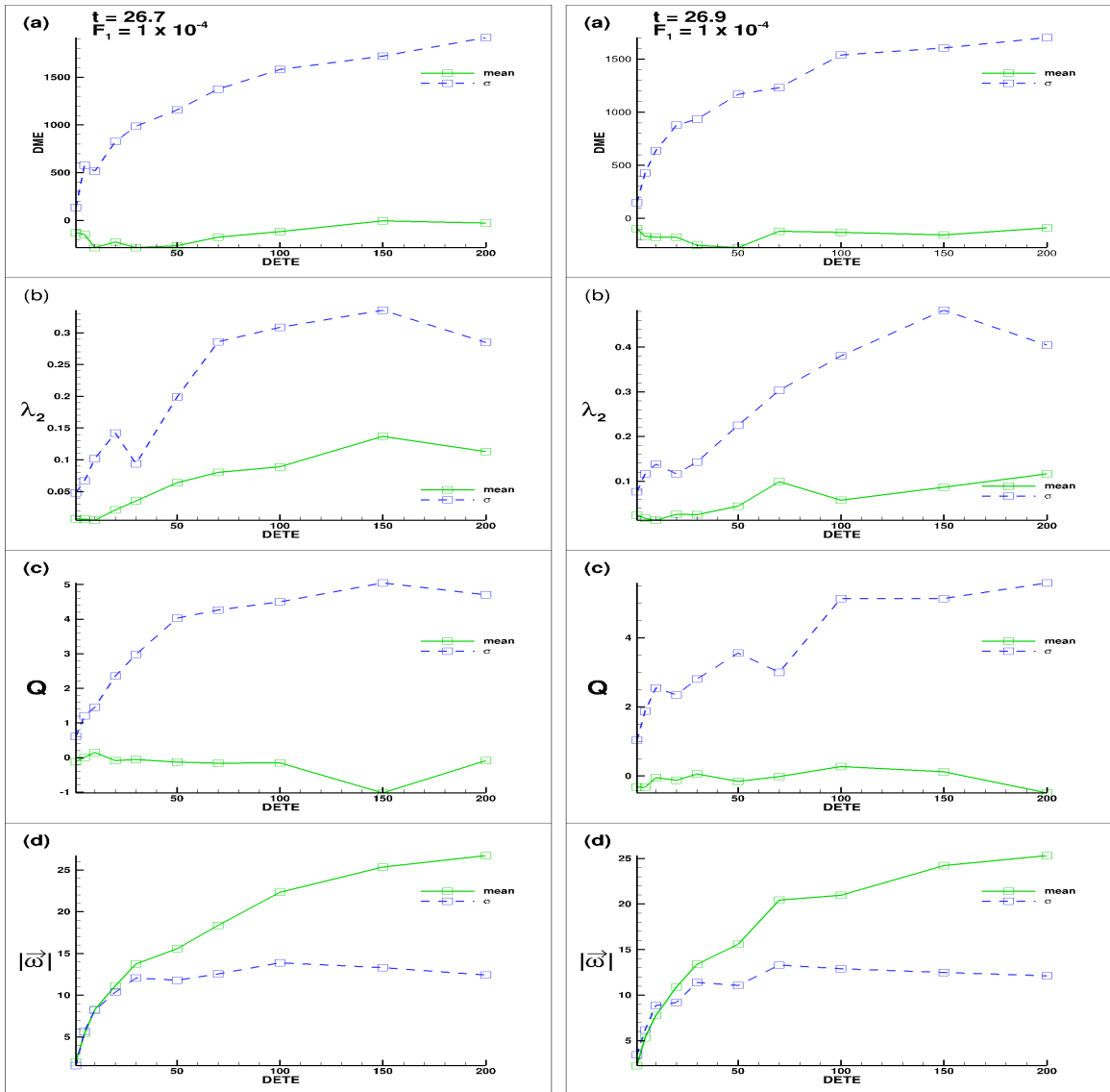


Figure 5.19: correlation of various criteria w.r.t DE TE

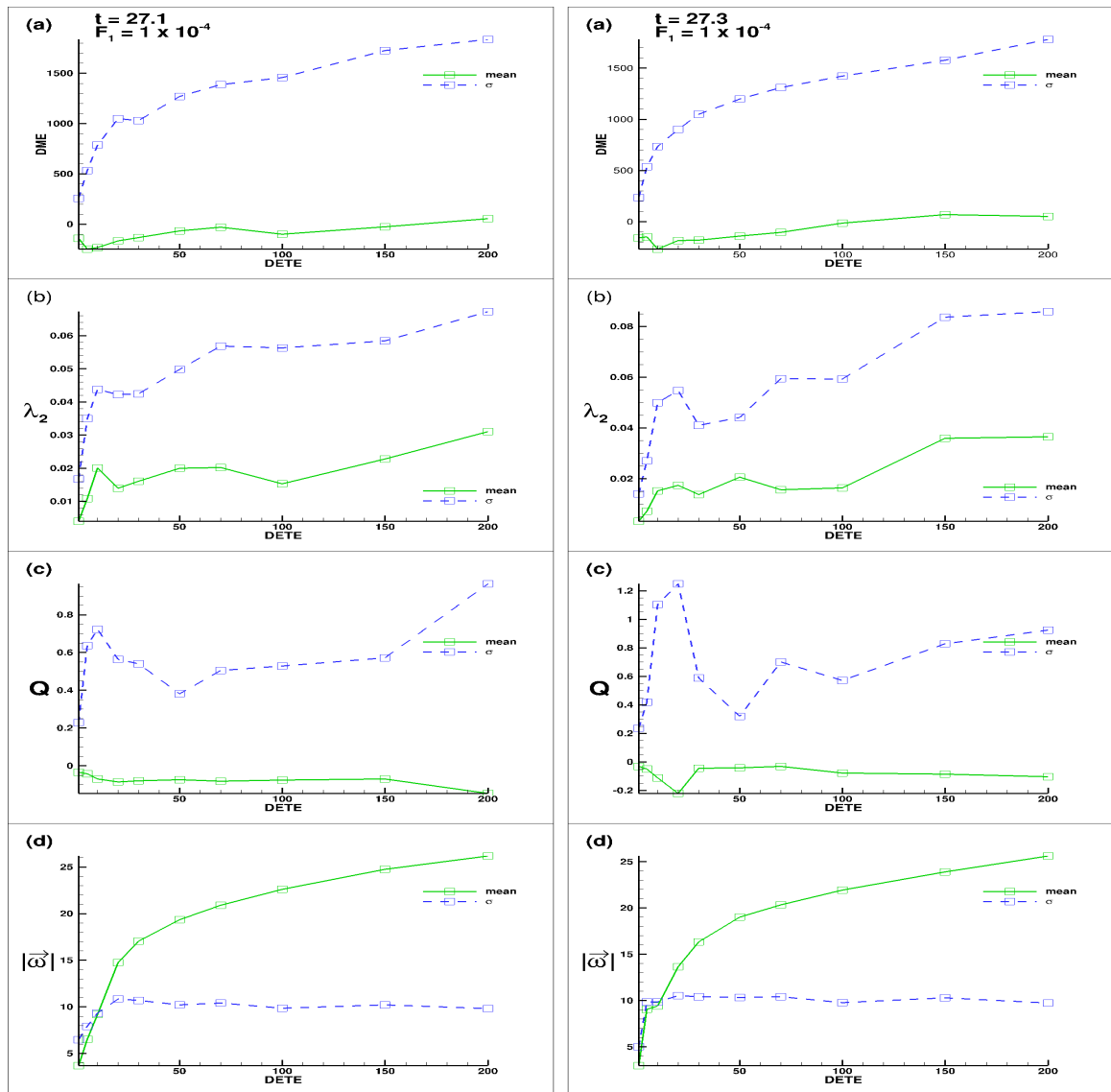


Figure 5.20: correlation of various criteria w.r.t DE TE

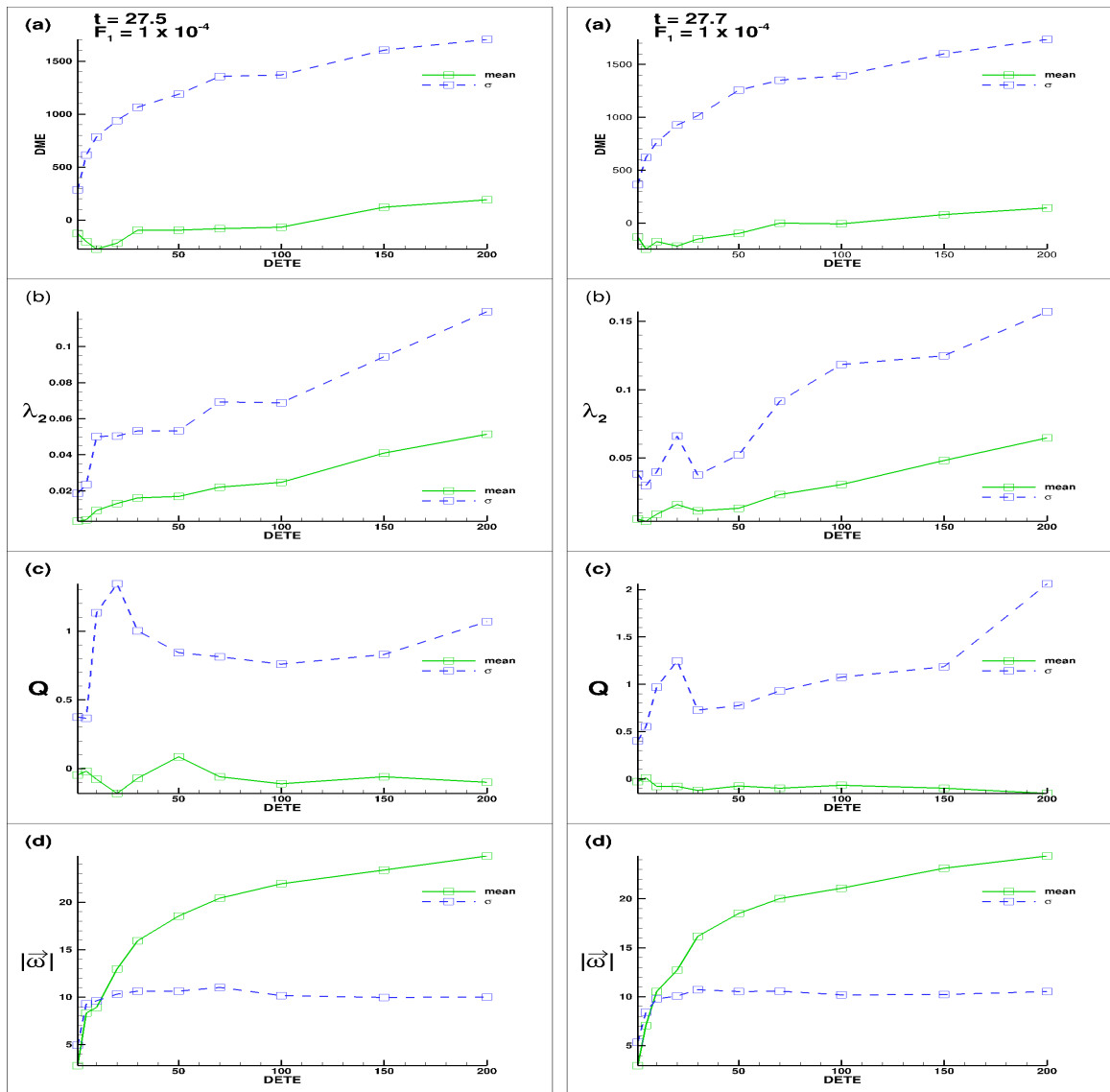


Figure 5.21: correlation of various criteria w.r.t DE TE

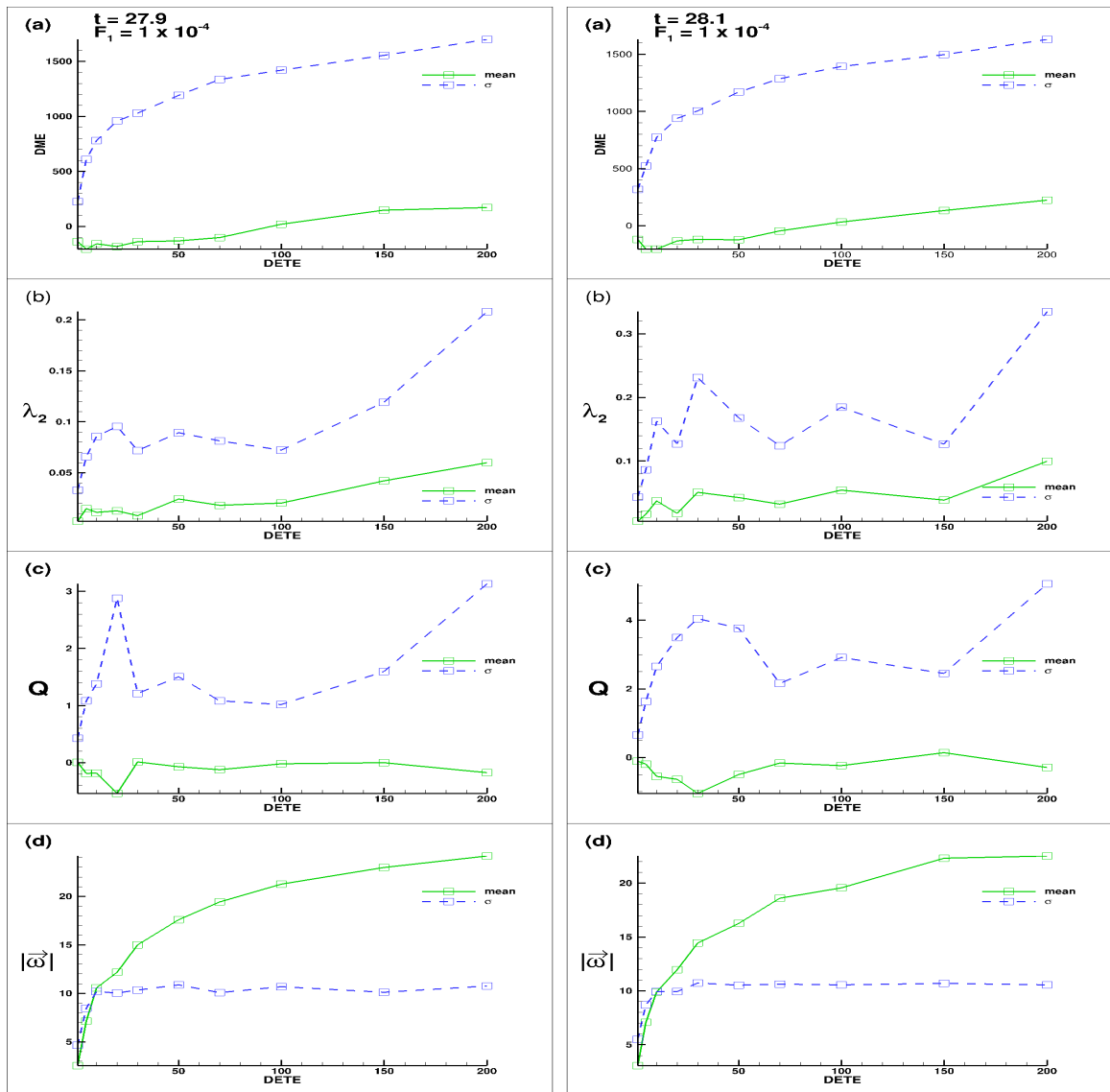


Figure 5.22: correlation of various criteria w.r.t DE TE

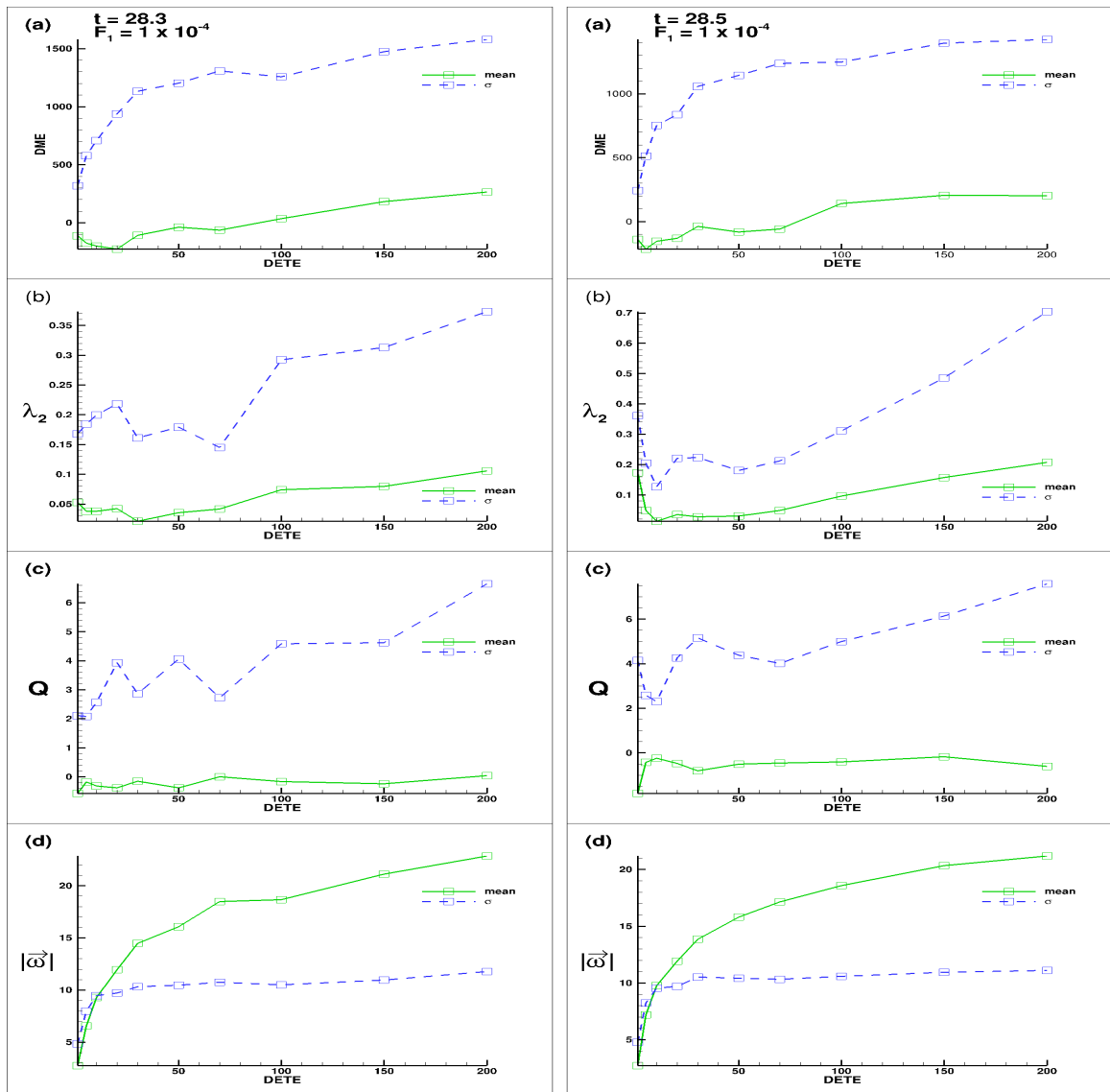


Figure 5.23: correlation of various criteria w.r.t DE TE

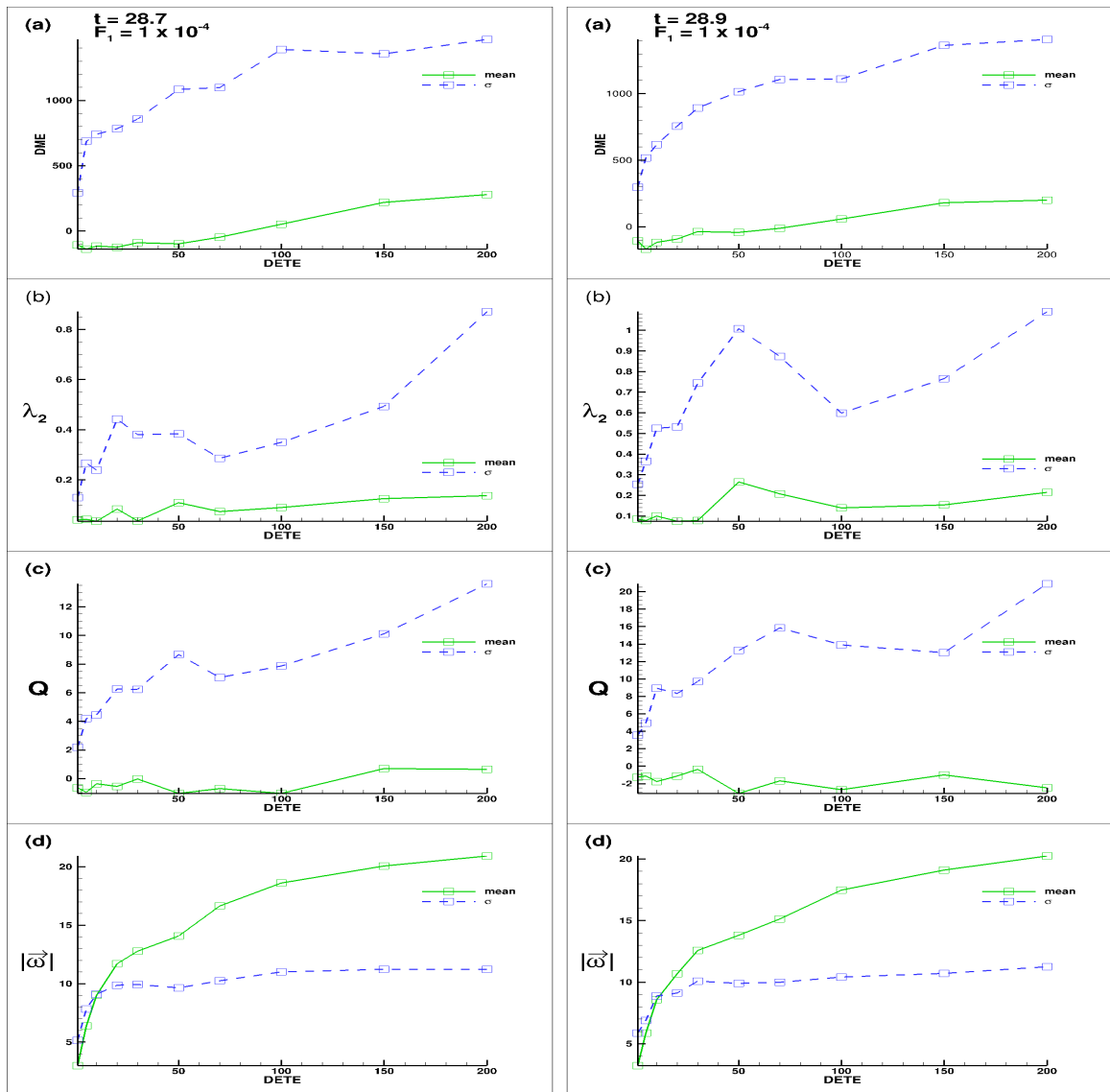


Figure 5.24: correlation of various criteria w.r.t DE TE



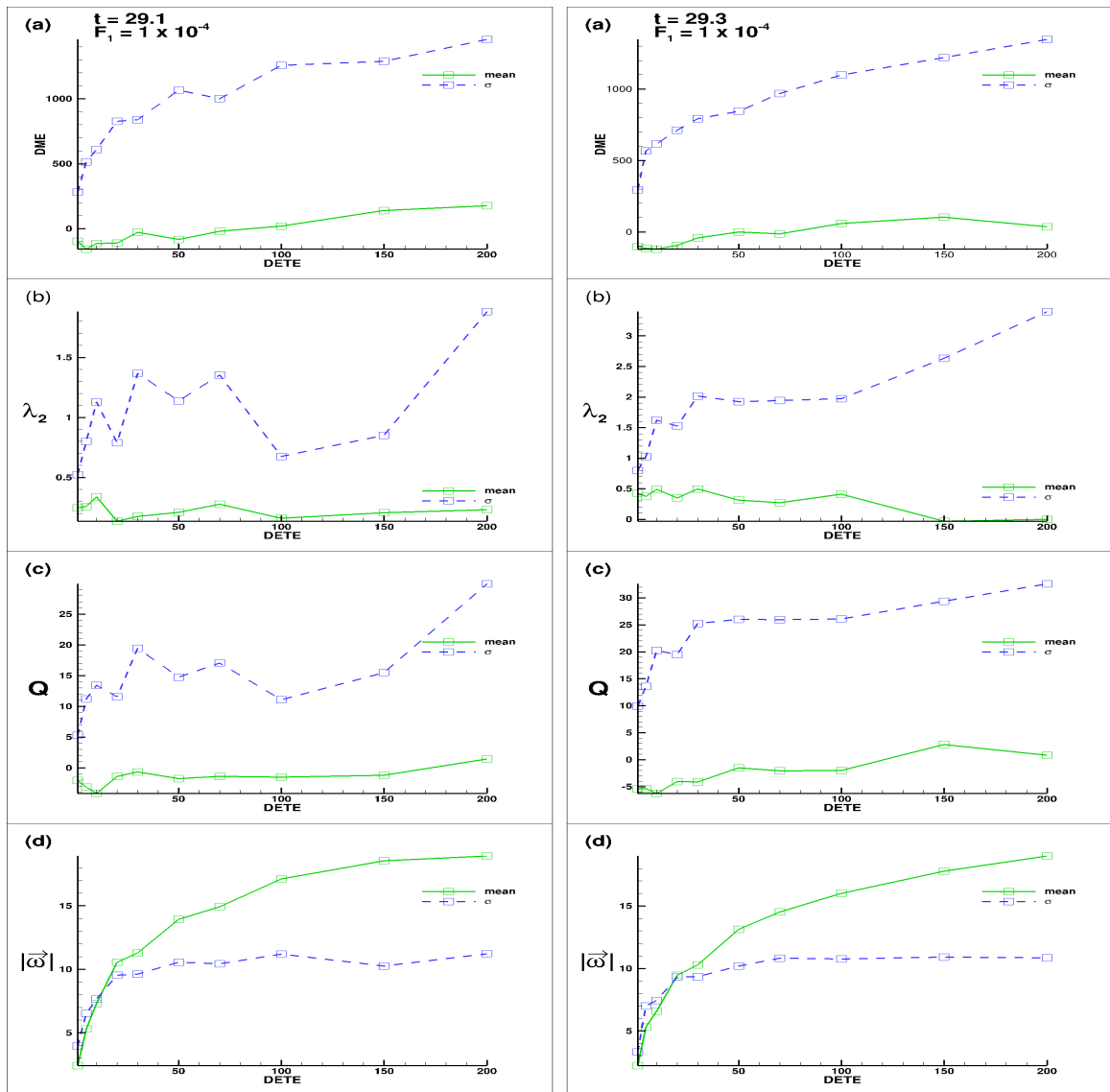


Figure 5.25: correlation of various criteria w.r.t DE TE

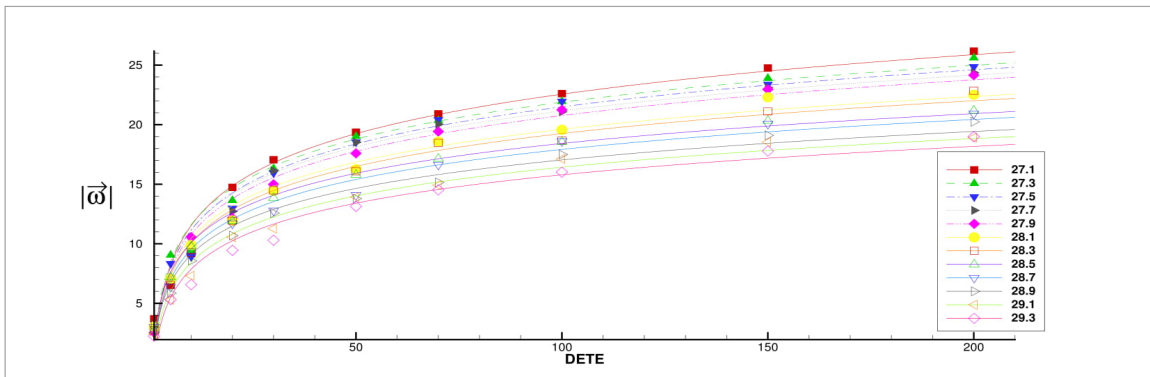


Figure 5.26: similarity of  $|\vec{\omega}|$  with DE TE for  $27.1 \leq t \leq 29.3$

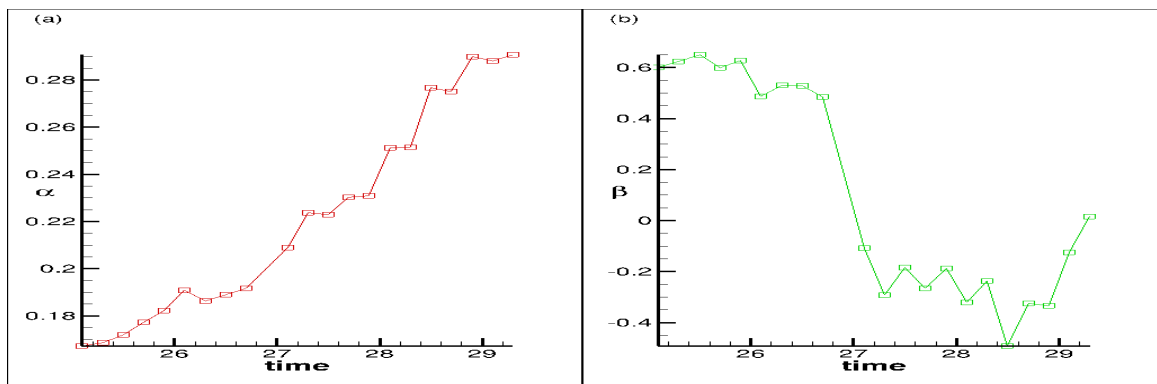
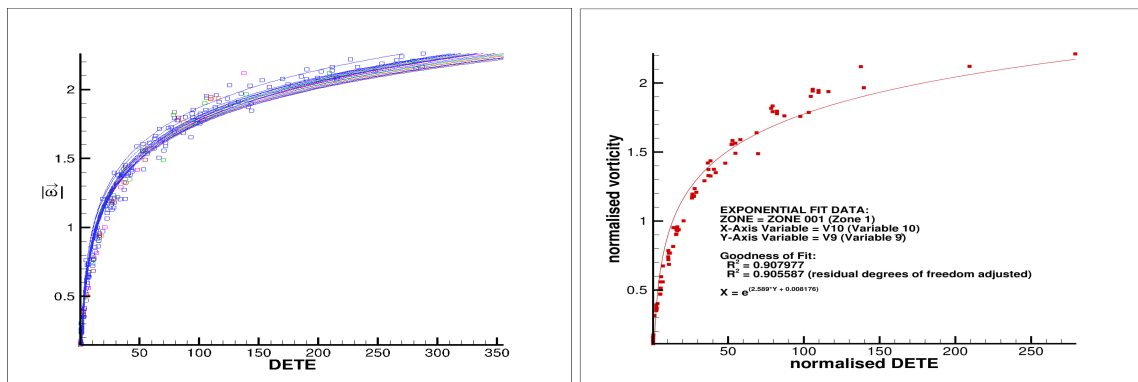


Figure 5.27: variation of  $\alpha$  and  $\beta$  of exponential fit with time



(a) exponential fits of scaled data for each time (b) exponential fit of scaled data for all time

Figure 5.28: exponential fit of scaled  $|\vec{\omega}|$  vs scaled DE TE.

# Bibliography

- [1] Liu C. Physics of turbulence generation and sustenance in a boundary layer. *Comput. Fluids*, 102:353, 2014.
- [2] J C. R. Hunt, Alan Wray, and Parviz Moin. Eddies, streams, and convergence zones in turbulent flows. *Center for Turbulence Research Report CTR-S88*, p.193–208.
- [3] Giuliano De Stefano, Filippo Maria Denaro, and Giorgio Riccardi. Analysis of 3-d backward-facing step incompressible flows via local average-based numerical procedure. *International Journal for Numerical Methods in Fluids*, 28:1073 – 1091, 11 1998.
- [4] Brenden Epps. Review of vortex identification methods. AIAA Paper 2017-0989, 2017.
- [5] Yisheng Gao and Chaoqun Liu. Rortex and comparison with eigenvalue-based vortex identification criteria. *Physics of Fluids*, 30(8):085107, 2018.
- [6] G. HALLER. An objective definition of a vortex. *Journal of Fluid Mechanics*, 525:1–26, 2005.
- [7] A. K. M. Fazole Hussain. Coherent structures and turbulence. *Journal of Fluid Mechanics*, 173:303–356, 1986.
- [8] Jinhee Jeong and Fazole Hussain. Hussain, f.: On the identification of a vortex. *jfm* 285, 69-94. *Journal of Fluid Mechanics*, 285:69 – 94, 02 1995.
- [9] Chaoqun Liu, Yisheng Gao, Shuling Tian, and Xiangrui Dong. Rortex—a new vortex vector definition and vorticity tensor and vector decompositions. *Physics of Fluids*, 30(3):035103, 2018.
- [10] Hans J. Lugt. *The Dilemma of Defining a Vortex*, pages 309–321. Springer Berlin Heidelberg, Berlin, Heidelberg, 1979.
- [11] Chakraborty P. On the relationships between local vortex identification schemes. *J. Fluid Mech.*, 535:189, 2005.

- [12] T. K. SENGUPTA, S. DE, and S. SARKAR. Vortex-induced instability of an incompressible wall-bounded shear layer. *Journal of Fluid Mechanics*, 493:277–286, 2003.
- [13] T. K. Sengupta, A. Kameswara Rao, and K. Venkatasubbaiah. Spatio-temporal growth of disturbances in a boundary layer and energy based receptivity analysis. *Physics of Fluids*, 18(9):094101, 2006.
- [14] Shuling Tian, Yisheng Gao, Xiangrui Dong, and Chaoqun Liu. Definitions of vortex vector and vortex. *Journal of Fluid Mechanics*, 849:312–339, 2018.
- [15] Kolář V. Vortex identification: New requirements and limitations. *Int. J. Heat Fluid Flow*, 28:638, 2007.
- [16] J. Jeong, F. Hussain, W. Schoppa, and J. Kim. Coherent structures near the wall in a turbulent channel flow. *Journal of Fluid Mechanics*, 332:185–214, 1997.
- [17] Bhaumik, S. and Sengupta, T. K. Precursor of transition to turbulence: Spatiotemporal wave front. *Phys. Rev. E.*, 89(4), 043018, 2014.
- [18] Bhaumik, S. and Sengupta, T. K. A new velocity-vorticity formulation for direct numerical simulation of 3D transitional and turbulent flows. *J. Comput. Phys.*, 284, 230-260, 2015.
- [19] Sharma, P., Sengupta, T. K. and Bhaumik, S. Three-dimensional transition of zero pressure gradient boundary layer by impulsively and nonimpulsively started harmonic wall excitation. *Phys. Rev. E.*, 98, 053106, 2018
- [20] M. K. Rajpoot, S. Bhaumik, and T. K. Sengupta Solution of linearized rotating shallow water equations by compact schemes with different grid-staggering strategies *J. Comput. Phys.* 231, 2300 (2012).
- [21] T. K. Sengupta, M. K. Rajpoot, and Y. G. Bhumkar Space-time discretizing optimal DRP schemes for flow and wave propagation problems *Comp. Fluids* 47, 144 (2011).
- [22] Aditi Sengupta, V. K. Suman, Tapan K. Sengupta, and Swagata Bhaumik. An enstrophy-based linear and nonlinear receptivity theory. *Physics of Fluids*, 30(5):054106, 2018.